Impact of regional climate change on the mosquito vector *Aedes albopictus* in a tropical island environment: La Réunion

K. Lamy [a,*], A. Tran [b], T. Portafaix [a], M.D. Leroux [c], T. Baldet [d]

[a] *LACy, Laboratoire de l'Atmosphère et des Cyclones (UMR 8105 CNRS, Université de La Réunion, Météo-France), Saint-Denis de La Réunion, France*
[b] *CIRAD, UMR TETIS, Sainte-Clotilde, La Réunion, France*
[c] *Météo-France, Direction Interrégionale pour l'Océan Indien, Saint-Denis de La Réunion, France*
[d] *ASTRE, Univ. Montpellier, Cirad, INRA, Sainte-Clotilde, La Réunion, France*

HIGHLIGHTS

- Climate change has a non-linear impact on precipitation in Reunion Island.
- The main type of breeding site modulates *Ae. Albopictus* sensitivity to climate change
- Both rainfall and temperature influence the distribution of *Aedes albopictus*.
- Climate change impact depends on scenario, season, region and altitude considered.

GRAPHICAL ABSTRACT
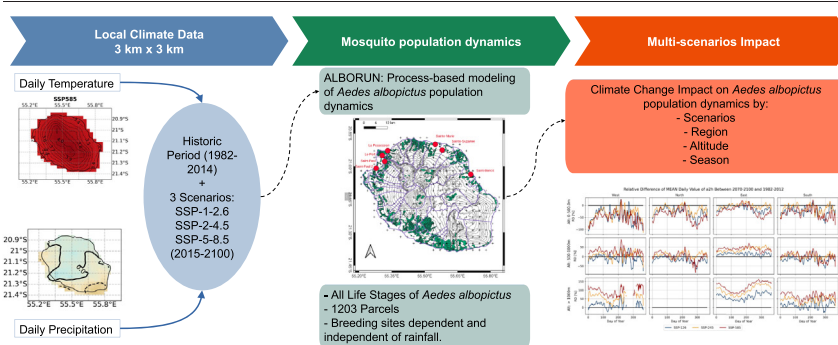
ARTICLE INFO

ABSTRACT

The recent expansion of *Aedes albopictus* across continents in both tropical and temperate regions and the exponential growth of dengue cases over the past 50 years represent a significant risk to human health. Although climate change is not the only factor responsible for the increase and spread of dengue cases worldwide, it might increase the risk of disease transmission at global and regional scale. Here we show that regional and local variations in climate can induce differential impacts on the abundance of *Ae. albopictus*. We use the instructive example of Réunion Island with its varied climatic and environmental conditions and benefiting from the availability of meteorological, climatic, entomological and epidemiological data. Temperature and precipitation data based on regional climate model simulations (3 km × 3 km) are used as inputs to a mosquito population model for three different climate emission scenarios. Our objective is to study the impact of climate change on the life cycle dynamics of *Ae. albopictus* in the 2070–2100 time horizon. Our results show the joint influence of temperature and precipitation on *Ae. albopictus* abundance as a function of elevation and geographical subregion. At low-elevations areas, decreasing precipitation is expected to have a negative impact on environmental carrying capacity and, consequently, on *Ae. albopictus* abundance. At mid- and high-elevations, decreasing precipitation is expected to be counterbalanced by a significant warming, leading to faster development rates at all life stages, and consequently increasing the abundance of this important dengue vector in 2070–2100.

1. Introduction

Vector-borne diseases (VBDs) are responsible for approximately 700,000 deaths per year and account for a significant proportion of the

* Corresponding author.
  E-mail address: kevin.lamy@univ-reunion.fr (K. Lamy).

global disease burden according to the World Health Organization (WHO) (World Health Organization, 2014). VBDs are caused by a variety of pathogens, including parasites, bacteria, and viruses, and are transmitted by arthropod vectors such as mosquitoes, ticks, flies, and fleas. Mosquitoes are particularly effective disease vectors, and while some diseases are now well-controlled or declining (e.g., malaria, lymphatic filariasis), others, such as arboviral diseases (e.g., dengue, chikungunya, zika or west Nile), are on the rise (Paixão et al., 2018). Dengue has grown exponentially over the last 50 years, with only 9 countries experiencing outbreaks before 1970 (Murray et al., 2013). Nowadays, dengue is present in >129 countries and is estimated to cause 390 million infections per year, including 96 million clinical cases and 40,000 deaths (Bhatt et al., 2013).

Several factors have been suggested to explain the recent spread of mosquito-borne viral diseases, such as global trade and travel (Gloria-Soria et al., 2014; Tatem et al., 2006), population growth (Struchiner et al., 2015), urbanization (Walker et al., 2011; Lowe et al., 2021; Lowe et al., 2020), environmental parameters (Kraemer et al., 2015; Kamal et al., 2018) and climate change (Kovats et al., 2001). Infected mosquitoes can be carried by humans in vehicles or container shipments (Eritja et al., 2017), but the pathogen is more commonly introduced to a new region through an infected host. Air travel has allowed the rapid spread of pathogens by returning travellers from endemic countries (Kilpatrick and Randolph, 2012; Semenza et al., 2014). *Aedes aegypti* and *Aedes albopictus*, key mosquito species in spreading diseases like dengue, chikungunya, and Zika, thrive near humans, especially in urban areas. *Ae. albopictus*, the tiger mosquito, has expanded globally in both tropical and temperate zones and *Ae. aegypti*, the yellow fever mosquito, is reappearing in former territories like the Mediterranean and southern US. *Ae. aegypti* is repopulating areas where it had previously been eradicated, including the Mediterranean region and the southern United States (Lwande, 2020). The breeding cycle, survival rate, and biting rate of mosquito vectors are all influenced by temperature, rainfall and humidity levels (Juliano, 2007). High ambient temperatures promote rapid vector development, increase the frequency of blood meals, and reduce the extrinsic incubation period (EIP), which is the duration between the time a virus is ingested by a vector and when it becomes capable of transmitting the disease. A short EIP increases transmission potential, while low temperatures reduce mosquito survival and limit transmission. Low ambient temperatures reduce the mosquito's survival rate and consequently their ability to become infectious and transmit the virus (Patz et al., 1998).

The global average surface temperature increased by 1.07 °C (0.8 to 1.3 °C) between the period 1850–1900 and 2011–2019 (IPCC, 2021). This increase is more pronounced over land, with a mean value of 1.59 °C (1.34 to 1.83 °C) (IPCC, 2021). Since the 1950s, global average rainfall has increased (IPCC, 2013), as well as the frequency and intensity of very heavy rainfall events (Bindoff, 2013; Knutson and Zeng, 2018; Wan et al., 2014). However, the effect of climate change on precipitation remains highly variable across geographical regions and seasons (Liu and Allan, 2013; Schurer et al., 2020). Additionally, the most recent global climate models (GCMs) forecast future rainfall conditions with significant variability. As a result, some regions are experiencing decreasing rainfall or increasing drought events both in terms of intensity and frequency (Bonfils et al., 2020; Li et al., 2015). The sixth iteration of the Coupled Model Intercomparison Project (CMIP6), a global collaborative climate projection exercise, incorporates Shared Socioeconomic Pathways (SSPs) (Meinshausen et al., 2020) to define the emissions scenarios. The optimistic (SSP-1-2.6), median (SSP-2-4.5), and pessimistic (SSP-5-8.5) scenarios predict global temperature increases of 1.8 °C, 2.7 °C, and 4.4 °C, respectively, between 1850–1900 and 2081–2100 (IPCC, 2021). Global average rainfall is expected to increase in high-latitude regions, the equatorial Pacific, and parts of the monsoon regions by 2081–2100. However, a decrease is expected in certain tropical and subtropical areas (IPCC, 2021; Solman and Orlanski, 2016; Chadwick et al., 2016). CMIP models still have systematic errors for annual tropical precipitation, but these errors have decreased from CMIP5/3 to CMIP6 (Tian and Dong, 2020).

Several studies have investigated the impact of current and future climate change on the transmission of VBDs. Messina et al. (2015) found that under the SSP-2 scenario, there could be an increase of 2.25 billion people at risk of dengue by 2080 (Messina et al., 2015). Liu-Helmersson et al. (2016) found that warmer temperatures in temperate regions like Europe could result in an increased risk of dengue outbreaks in southern European cities by 2100 (Liu-Helmersson et al., 2016). Based on the representative concentration pathways (RCPs), the previous-generation climate scenarios, Ryan et al. (2018) determined that the risk of vector-borne disease transmission due to climate change would increase significantly for Europe and decrease in West Africa and Southeast Asia by 2070 compared to the period 1970–1999 (Ryan et al., 2018). Iwamura et al. (2020) showed that the world became 1.5 % more sustainable for mosquito life cycle renewal each decade from 1950 to 2000 and that this trend would accelerate to 3.2 % and 4.4 % by 2050 under RCP4.5 and RCP8.5 scenarios, respectively (Iwamura et al., 2020). Based on the SSP scenarios, Colón-González et al. (2021) found that the duration of the malaria transmission will increase in the African highlands, the eastern Mediterranean and some parts of the Americas. Similarly, the dengue transmission months season will increase in the eastern Mediterranean and the western Pacific (Colón-González et al., 2021). Bonnin et al. (2022) recently found increased densities of *Ae. albopictus* and *Ae. aegypti* with locally contrasted seasonal responses by the end of the century in Southeast Asia (Lucas et al., 2022).

The aforementioned studies provide information on global trends, but the spatial resolutions of the global climate models (GCMs) used may be on the order of hundreds of kilometers. Meanwhile, factors that impact mosquito populations occur at a finer scale (Sauer et al., 2021; Murdock et al., 2017; Li et al., 2014). Mosquito abundance and distribution are influenced by the flight range of adult females (Vavassori et al., 2019) and the availability of suitable habitats (Sauer et al., 2021; Brown et al., 2017), both of which are shaped by local environmental and microclimatic factors such as building density, residual heat, standing water sources, and vegetation cover (Larsen, 2015; Kumar et al., 2018). These small-scale factors can challenge the accuracy of models predicting local mosquito population dynamics and associated disease transmission risk (Faridah et al., 2022). This issue can be exacerbated in regions with contrasting or heterogeneous microclimates or environments such as Réunion Island in the southwestern Indian Ocean. This mountainous island has a large number of microclimates (Jumaux et al., 2011), ranging from very arid to very humid habitat types (Strasberg et al., 2005), a maximum elevation of 3000 m asl and a population of >800,000 (Insee, 2022). Réunion Island has experienced several arbovirus epidemics, including dengue (1977–1978) (Coulanges et al., 1979) and chikungunya (2005–2006) (Schuffenecker et al., 2006; Kles et al., 1994), both spread by *Ae. albopictus*. Dengue circulation was sporadic until a major and ongoing epidemic started in 2017, involving the circulation of three dengue virus serotypes (DENV-1, DENV-2 and DENV-3) and resulting in increased cases, including severe forms and deaths (Vincent et al., 2019; Hafsia et al., 2022). A mechanistic numerical model of *Ae. albopictus* population dynamics ('ALBORUN') has recently been developed and validated for Réunion Island (Tran et al., 2020). In addition, high-resolution climate projections were carried out as part of the Building Resilience in the Indian Ocean (BRIO) project to improve the assessment of climate change risks in the small islands of the southwestern Indian Ocean (Leroux, 2021).

What is the impact of climate change on mosquito populations and dengue epidemics at a local scale, and how do environmental and climatic conditions contribute to this relationship? To answer this question, we can use the variety of environmental and climatic conditions and the availability of high-quality meteorological, entomological, and epidemiological data on the island. We used climate projections from the BRIO project, which have been downscaled to a 3-km resolution for three scenarios (SSP-1-2.6, SSP-2-4.5, and SSP-5-8.5), as inputs for the ALBORUN model.

In the following section, we present the entomological and epidemiological data, climate models, and the mosquito population dynamics model. In the third section, we present the climate projections and validate the results of the coupling of BRIO and ALBORUN. Lastly, we examine the

expected future climate outcomes by 2070–2100 under the three SSP scenarios and the impact of climate variables on the life cycle and population dynamics of *Ae. albopictus*, the main dengue vector on the island.

2. Methods, data and models

2.1. Data

2.1.1. Entomological data

The Regional Health Agency of Réunion Island (ARS Réunion), responsible for vector control activities, has set up a detailed monitoring of *Ae. albopictus* population dynamics. This monitoring confirms the strong spatial and temporal heterogeneities of the dengue vector (Vincent et al., 2019; Hafsia et al., 2022). The ALBORUN model allows one to define the vector risk on the territory of Réunion Island to orientate preventive control and surveillance actions in high-risk areas. ALBORUN is now an operational tool used by ARS Réunion to generate predictive maps of tiger mosquito density on a weekly basis based on temperature and rainfall data collected by Météo-France Réunion.

Monitoring of *Ae. albopictus* populations and vector control interventions around reported dengue cases are organized through the treatment of areas where dengue cases have been reported are distributed throughout 1203 operational zones, called 'ALIZES' parcels (Fig. 1). In each of these zones, the rainfall-dependent environmental carrying capacity of larvae and pupae (Kl/p,var) and the rainfall-independent environmental carrying capacity of larvae and pupae (Kl/p,fix) are determined from entomological field surveys. These surveys, carried out in several zones that are representative of the different environmental and climatic contexts of the island, make it possible to quantify the number and type of breeding sites (generally consisting of small containers filled with water where *Ae. albopictus* females lay their eggs) and the average number of larvae or pupa observed per breeding site in each zone. In addition, trapping of adult mosquitoes using Biogents sentinel traps™ (Kröckel et al., 2006) and collection of mosquito eggs or larvae using oviposition traps (Focks, 2003) were carried out extensively between 2012 and 2013 and between 2018 and 2020. Each trapping site is representative of an area with a radius of approximately 300 m, corresponding to the flight range of *Ae. albopictus* (Lacroix et al., 2009). More details on the calculation of carrying capacities and the methodology used for these traps and mosquito population counts are available in Tran et al. (2020).

2.1.2. Meteorological data

Météo-France (the French national weather service) has a dense observation network of weather stations spread over the island. These stations record several meteorological parameters, including precipitation and temperature. Stations with sufficiently long and homogenised time series were used herein to correct the model bias. Seventy-six stations were used to correct for precipitation bias, and 20 stations were used to correct for temperature bias. Using a simple kriging method (Oliver and Webster, 1990), these observations were reinterpolated to a 3-km × 3-km grid. These data will hereafter be referred to as OBS-BRIO. Then, the OBS-BRIO data were used to adjust the climate simulations produced by ALADIN-climate and carried out in the framework of the BRIO project. The 'ALIZES' parcels and their corresponding weather model grid points were classified into three elevation categories: low elevation (0–500 m asl), medium elevation (500–1000 m asl) and high elevation (above 1500 m asl). To analyse seasonal variations, four standard seasons were defined: December, January and February (DJF); March, April and May (MAM); June, July and August (JJA); and September, October, November (SON). Finally, to investigate spatial variations, these same parcels were grouped into four regions: eastern, northern, southern and western regions.
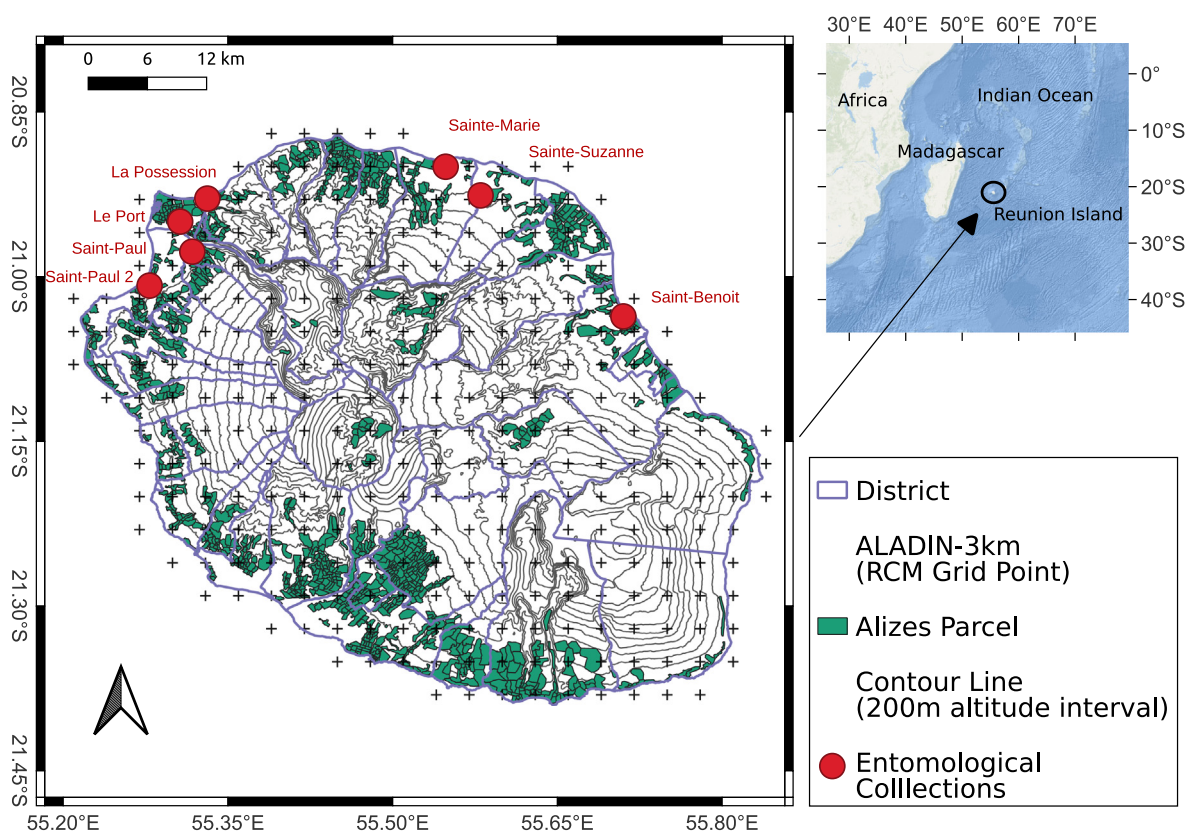

Fig. 1. Map of Réunion Island depicting the observation data. The RCM grid points are represented by black crosses. The ALIZES parcels are represented by green polygons. The 200-m iso-elevation intervals are represented by grey lines. Districts where dengue cases may have been recorded are delimited by blue contours. Locations of the entomological collections used to validate the method are indicated with red circles. (For interpretation of the references to color in this figure legend, the reader is referred to the web version of this article.)

2.1.3. Epidemiological data

Epidemiological surveillance of dengue is carried out weekly for each commune on the island by Santé Publique France, the National Public Health Agency. The good quality and spatial coverage of this dataset allows one to characterise the epidemiology of dengue fever on the island, which is characterized by strong seasonal and spatial variabilities. Epidemic peaks are classically observed between March and June, corresponding to the end of the austral summer, when conditions are typically hot and humid; then, cases gradually decrease from June to July during the austral winter. Dengue circulation has been maintained during the austral winter since 2017 (Santé Publique France, 2021). This persistence of dengue during the interepidemic period is a recent trend that may favour a rapid increase in cases early in the year and an increased risk of imported cases into southern Europe at times when *Ae. albopictus* populations are abundant. The 2016–2020 epidemics show concentrations of dengue cases in the southern and western regions of the island (Santé Publique France, 2022). Several factors related to dengue genotypes, human populations, mosquito vectors, environmental and meteorological factors, as well as interactions between these factors, may explain the spatiotemporal distribution of dengue cases observed in Réunion Island in recent years. Weekly dengue cases confirmed by Santé Publique France between 2017 and 2021 were aggregated according to their district-scale distribution.

2.2. Model

2.2.1. The ALBORUN model

ALBORUN is a mechanistic and phenological model originally designed to simulate the population dynamics of the mosquito vector *Ae. albopictus*. First developed for the south of France (Cailly et al., 2012), the model was subsequently adapted for the territory of Réunion Island. This model solves a system of ordinary differential equations (ODE) describing the different life stages of the mosquito: its aquatic stages (eggs, larvae and pupae) and adult stages (hereafter referred to as A_1 or A_2, where A_1 refers to nulliparous females that have never laid eggs and A_2 refers to parous females that have laid eggs at least once), including host-seeking females (hereafter referred to as A_{1H} or A_{2H}), gravid females that are ready to lay eggs (hereafter referred to as A_{1G} or A_{2G}) and ovipositing females (hereafter referred to as A_{1O} or A_{2O}). The ODE system predicts mosquito abundance by stage based on constant parameters (male/female ratio, number of eggs laid, minimum temperature for egg development, etc.) and dynamic weather dependent parameters (temperature-dependent transition functions between stages, mortality rates of different stages, etc.). A brief description of the variables is given in Table 1. Complete parameter setting can be found in Tran et al. (2020).

For the present study, it is noteworthy that the transition functions from egg to larvae, larvae to pupa, pupa to adult and gravid adult to ovipositing adult are all temperature dependent. The transition function from oviposition to host-seeking is rain dependent, as this transition depends on the availability of oviposition sites and, thus, on the carrying capacity of the environment. Egg mortality is rain dependent; if rainfall is too heavy,

breeding sites can be flushed away. Larval and pupal mortality are mainly temperature dependent, but again, if rainfall exceeds a particular threshold, breeding sites will be washed away. Rainfall is thus a critical variable in mosquito population dynamics because its effects are nonlinear. Finally, adult mortality rate is temperature dependent. The temperature (T) used in the calculation of these functions is the daily average temperature (T_{mean}, see Table 1). More details on the formulations of these transition functions and mortality rates are provided in Tran et al. (2020) and adapted from Delatte et al. (2009). A summary of these functions and their dependence on meteorological variables is presented in Table 2.

2.2.2. Climate modelling

The climate projections used in this study were obtained from simulations performed as part of the BRIO project (Leroux, 2021). The simulations analyzed different combinations of socioeconomic scenarios and greenhouse gas emission pathways using several GCMs or Earth System Models (ESMs). ESMs are designed to account for additional processes that impact general circulation and atmospheric chemistry, such as ocean ecology and biogeochemistry, plant ecology, land use, and continental ice sheets. CMIP6 outputs from the CNRM-ESM-2-1 (Séférian et al., 2019; Séférian et al., 2016) were used as forcings for the regional limited-area model ALADIN (with a 12-km spatial resolution) (Daniel et al., 2018; Nabat et al., 2020). Both models were developed by the Centre National de Recherche Météorologiques (CNRM), Toulouse, France. Gridded observations from ground-based networks over La Réunion (OBS-BRIO) were used to bias-correct the data over the historical period and perform statistical downscaling (Michelangeli et al., 2009; Vrac et al., 2012). The historical period of the simulations spans 1981–2014, while the future period range between 2015 and 2100 under three climate scenarios (SSP-1-2.6, SSP-2.4.5 and SSP-5-8.5) (O'Neill et al., 2016).

An additional scenario is realized: SSP-5.85-Tfix. In this scenario, temperatures are "fixed" at historical levels. To do this, the climatological temperature anomaly is removed from the time series of each grid point, thus retaining the natural climate variability but removing the tendency to increase.

2.2.3. ALBORUN simulations

Maximum and minimum daily temperature and daily rainfall data simulated by ALADIN-Climate and downscaled to a 3-km resolution were used as input data for the ALBORUN model. For each ALIZES parcel in ALBORUN, the model grid point closest to the corresponding ALADIN-Climate output was used (Fig. 1). This process was carried out for the historical period and for the three future SSP scenarios. In order to focus on the long-term anthropogenic climate signal, 30-year climatological averages were used to filter out natural climate variability. Long-term averages were calculated for the historical period (1982–2012) and the future period (2070–2100). A 30-year running average was also used over the period 2005–2085. Because not all parcels have the same total environmental (rain-dependent and rain-independent) carrying capacity, it was necessary to normalise the resulting values to allow comparisons of the parcels. Therefore, the amplitudes of the modelled values in each ALIZES parcel were normalised by the maxima and minima modelled in each parcel over the entire modelling period (1980–2100).

2.3. Model validation

Climate models have the ability to reproduce seasonal or regional climate variability but cannot reproduce the observed weather at a specific date. To validate the consistency of our results, we therefore used data (OBS-BRIO) from the same weather stations as those used to debias the ALADIN climate simulations. These observations (minimum and maximum temperature and daily rainfall), on a 3-km grid, were used as inputs to the ALBORUN model for the 2000–2020 period.

2.3.1. Historical validation against entomological data

The results of this integration (hereafter referred to as OBS-BRIO-ALBORUN) were then compared to entomological observations of *Ae.*

Table 1

Description of the entomological and meteorological variables used in the ALBORUN Model.

Variable notation	Definition
T_{max}	Daily minimal temperature
T_{min}	Daily maximal temperature
T_{mean}	Daily average temperature ($T_{max} + T_{min}$)/2
Rain	Daily rain accumulation
Washout	Sharp increase of aquatic stages mortality rate if rain >80 mm
7 last days with rain	Number of days with at least 10 mm of rain during the last 7 days
Env. capacity	Environmental carrying capacity
A1H	Nulliparous host-seeking female mosquito
A1G	Engorged to gravid transition for nulliparous female mosquito
A1O	Oviposition site-seeking female mosquito
A2H	Parous host-seeking female mosquito
A2G	Engorged to gravid transition for nulliparous female mosquito
A2O	Oviposition site-seeking female mosquito

Table 2

Summary of the functions used in the ALBORUN model and their dependence on meteorological variables. T: Temperature (°C), T_E: Minimal temperature needed for egg development (°C), TDD_E: Total number of degree-day necessary for egg development (°C), T_{ag}: Minimal temperature needed for egg maturation (°C), TDD_{Ag}: Total number of degree-day necessary for egg maturation (°C) Rain: Precipitation (mm), γ_{Ao}: Minimum transition rate from ovipositing to host-seeking adults (day-1), μ_E: Minimum egg mortality rate (day-1).

ALBORUN model functions		Function	Reference
Transition function	Egg to larva	$\begin{cases} T(t) - T_E/TDD_E & \text{if } T(t) > T_E \\ 0 & \text{otherwise} \end{cases}$	(Tran et al., 2013)
	Larva to pupa	$q_1 T^2 + q_2 T + q_3$ with $q_1 = -0.0007$, $q_2 = 0.0392$, $q_3 = -0.3911$	(Tran et al., 2013)
	Pupa to emerging adult	$q'_1 T^2 + q'_2 T + q'_3$ with $q_1' = -0.0008$, $q_2' = 0.0051$, $q_3 = -0.0319$	(Tran et al., 2013)
	Engorged adult to oviposition site-seeking adult	$\frac{T(t) - T_{Ag}}{TDD_{Ag}}$	(Tran et al., 2013)
	Ovipositing to host-seeking adults (day^{-1})	$\gamma_{AO}(1 + Rain_{norm})$	(Pachka, 2016)
Mortality rate	Egg	$\begin{cases} \mu_E & \text{if } Rain > 80 \\ 0 & \text{otherwise} \end{cases}$	(Tran et al., 2013; Dieng et al., 2012)
	Larva	$0.02 + 0.0007e^{0.1838(T-10)} + \begin{cases} 0.5 & \text{if } Rain > 80 \\ 0 & \text{otherwise} \end{cases}$	(Delatte et al., 2009; Dieng et al., 2012)
	Pupa	$0.02 + 0.0003e^{0.2228(T-10)} + \begin{cases} 0.5 & \text{if } Rain > 80 \\ 0 & \text{otherwise} \end{cases}$	(Delatte et al., 2009; Dieng et al., 2012)
	Adult	$0.025 + 0.0003e^{0.1745(T-10)}$	(Delatte et al., 2009)

albopictus eggs, larvae and adult females carried out by ARS Réunion at different periods (Fig. 2).

As shown in Fig. 2, seasonal and interannual decreases and increases are well correlated between OBS-BRIO-ALBO and ALBORUN. For 5 of the 8 study sites, Spearman correlation coefficients are high ($r > 0.5$) and significant. Tran et al. (2020) obtained very similar results using in situ data from weather stations. This is consistent with the fact that these same weather stations were used to construct the gridded weather observations used here. Trapping was carried out over periods ranging from a few months

to a maximum of two years. The amplitudes of the changes observed from these samples are therefore not as representative as those observed on the ALIZES parcel series from ALBORUN. These discrepancies could explain the differences between the two results, especially for the St-Benoit (larvae) and Le Port (eggs) sites.

2.3.2. Historical validation against dengue cases data

Dengue epidemiological monitoring data collected in each district between 2017 and 2020 by Santé Publique France were also compared to
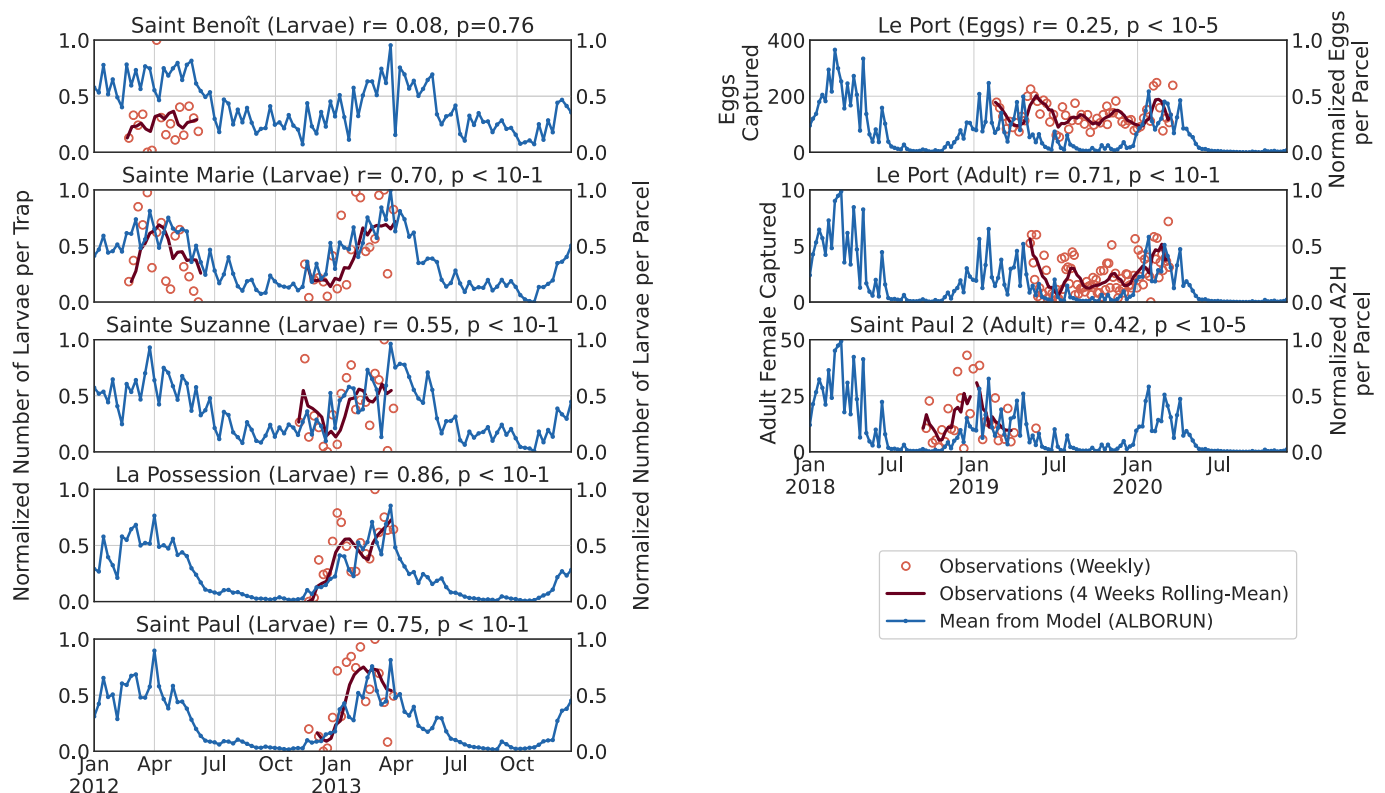

Fig. 2. Observed and modelled larvae, eggs and adult for 7 different sites in Réunion Island. Entomological observations made by trapping are represented by red circles. The simulated numbers of eggs, larvae or adult females modelled by ALBORUN in each ALIZES parcel located within a 3-km radius (for consistency with the resolution of the meteorological data) around sampling sites are represented by blue lines. The weekly total capture numbers are represented by red circles, and the 4-week moving average of the total capture numbers are represented by dark red lines. (For interpretation of the references to color in this figure legend, the reader is referred to the web version of this article.)

the average evolution of the A2H variable in the corresponding ALIZES parcels (Fig. 3). The A2H variable was chosen because it corresponds to host-seeking female mosquitos that have already taken at least one blood meal and therefore represent potential dengue vectors. In Fig. 3, we can see that the occurrence of dengue cases is always correlated with the A2H variable in the different districts. It should be noted that a decrease in dengue cases after an epidemic peak is almost always preceded (by a few days) or accompanied by a decrease in the A2H variable in the corresponding district. Furthermore, even if the number of cases in a district is low (i.e., a value less than twenty appears in the second row) or very low (a value less than ten appears in the first row), these cases always appear with high A2H values and disappear when the A2H variable decreases. These results show the coherence and relevance of the ALBORUN model for monitoring, forecasting and modelling the epidemiological dynamics of dengue in Réunion Island. Moreover, this result allows us to confirm that it is reasonable to use the A2H variable (representing host-seeking parous mosquito females) as a proxy instead of dengue cases to quantify the possible epidemiological dynamics of dengue. Although it cannot be said that the presence of A2H is equivalent to the presence of dengue cases, the presence of A2H remains a necessary condition for dengue, and the magnitude of the A2H variable appears to have a direct impact on dengue epidemic dynamics.

The scale of the number of dengue cases (on the right axis) is not the same for each row. Some districts had only a dozen cases, while others had hundreds. For some districts, no corresponding ALIZES parcels were modelled, so it was not possible to represent the A2H variable in these districts. For each district and year, we calculated the lag that maximized the correlation between the peak abundance of A2H and the peak of dengue cases. We then took the average of the calculated lags and obtained a value of approximately 48.04 days. This result is very interesting. One might think that the time difference between these two peaks would be

the sum of the extrinsic incubation period in the mosquito vector and the intrinsic incubation period in the human host (2–15 days at 30 °C for the EIP and 5.9 days for the IIP (Chan and Johansson, 2012) or about 7.9–20.9 days). Nevertheless, our result suggests that the epidemic peak is delayed by an additional twenty days approximately. We can assume that this is due to the time needed for an amplification of the epidemic process in the human population. Although studies examining the temporal relationship between mosquito vector abundance and dengue incidence are still rare, some recent research performed in Guangzhou (China) have shown a time lag of at least one month between the peak of *Ae. albopictus* vector abundance and the peak of dengue cases (Xu et al., 2017).

3. Results

3.1. Climate simulation

3.1.1. Temperature response to climate change

The absolute differences between the 2070–2100 period and the 1982–2012 period for three SSP climatic scenarios are presented in Fig. 4.

Temperatures show a linear response to climate scenarios. The higher the radiative forcing, the higher the temperatures in 2070–2100. For a radiative forcing of 2.6 W·m^{-2} (SSP-1-2.6), an increase in mean annual temperature of approximately 1 °C is expected over the whole island. This increase in mean annual temperatures is on the order of approximately 2 °C under SSP-2-4.5 and about 3.5 °C to 5 °C under SSP-5-8.5. Overall, the largest temperature increase is simulated over the central highland region under all three SSP climates. Moreover, the gradient of the temperature difference (space between the isolines) is greater under SSP-5-8.5 (+3.2 °C on the coast and approximately +4.0° in the higher parts of the island) which corresponds to a temperature difference gradient of approximately 0.3 °C per km. For SSP-1-2.6, there is a temperature difference gradient of
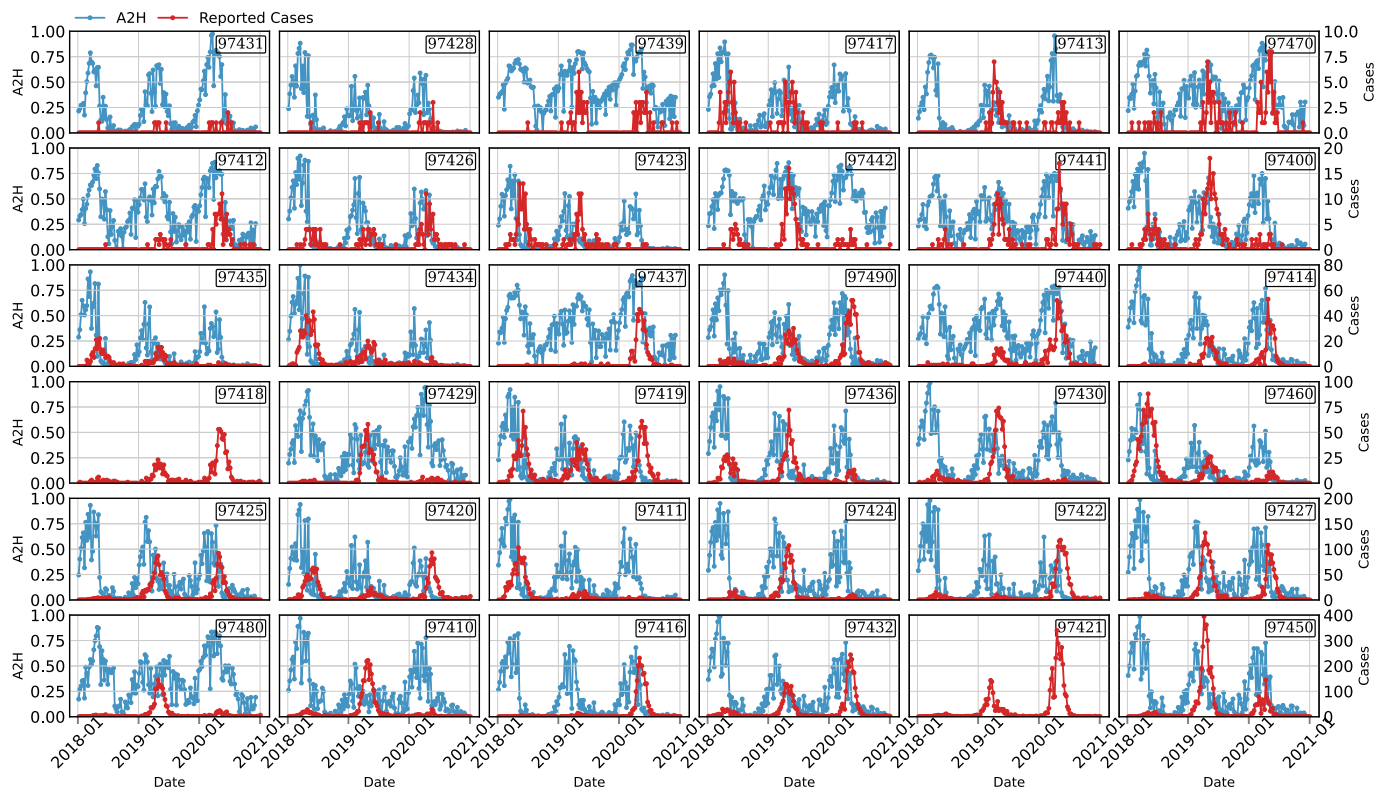

Fig. 3. Number of reported dengue cases and normalised number of host-seeking females Aedes (A$_{2H}$) modelled by district. The numbers of reported dengue cases are represented by the blue curves. The numbers of A2H (normalised between 0 and 1) modelled by ALBORUN are represented by the blue curves. The postal codes of the different districts are indicated in the upper right-hand corner of each subplot. The vertical scale of the number of dengue cases is the same for each line but differs from one line to another to avoid figures compression. (For interpretation of the references to color in this figure legend, the reader is referred to the web version of this article.)
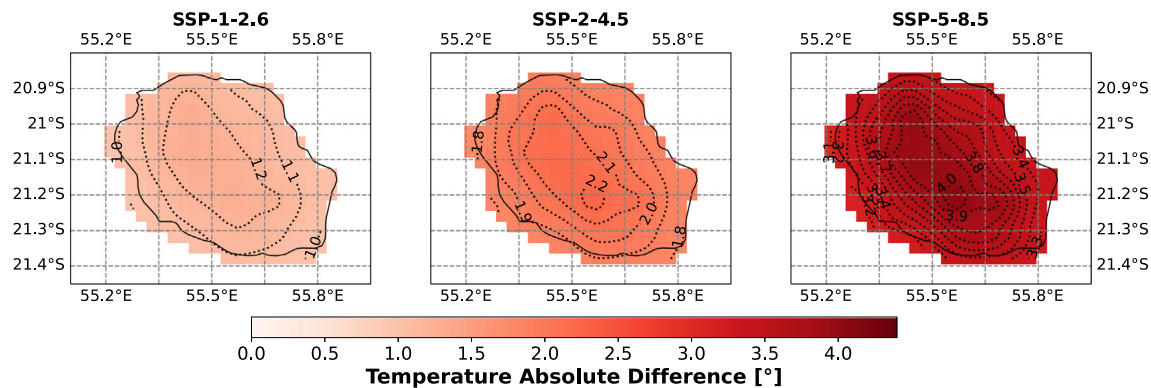
Fig. 4. Absolute differences in temperature between the 2070–2100 and 1982–2012 periods. Isolines indicating temperature differences of 0.1° are shown as dotted lines.

approximately 0.1° per km (+1.1 °C on the coast and approximately +1.3 °C in the higher parts of the island).

3.1.2. Rainfall response to climate change

Regarding precipitation, the relative differences between the 2070–2100 and the 1982–2012 climatological periods under the three SSP climatic scenarios and for the four seasons were calculated and are represented in Fig. 5.

Unlike the temperature results, the precipitation results do not exhibit any linear relationship with the magnitude of the climate scenario. Considering the MAM season, under the SSP1-2.6 scenario, by 2070–2100, this season was predicted to be drier over most of the island than in the historical period (approximately −10 % to −20 % rainfall). For the same season, the SSP2-4.5 scenario shows a zonal dipole, with relatively dry conditions in the west and relatively wet conditions in the east. Finally, under the SSP5-8.5 scenario, the same season (MAM) will be approximately 10 to 40 % drier by the end of the 21st century. There does not appear to be any linear relationship between the magnitude of the expected radiative forcing and changes in precipitation. However, it can be noted that, overall, the SSP5-8.5 scenario shows the most pronounced drying. Finally, in contrast to the other seasons, the DJF season is the only season that shows a slight positive precipitation trend regardless of the climate scenario.

3.2. ALADIN-ALBORUN simulation

3.2.1. Expected climate change at the end of the 21st century

The relative differences in the A2H variable between the 2070–2100 and 1982–2012 climatological periods in each ALIZES parcel, under the three SSP climatic scenarios and in all four seasons were calculated. The mean climatological relative differences are represented in Fig. 6.

In general, coastal areas appear to dominate, showing decreases of 10–20 % in the A_{2H} variable by 2070–2100 in all three climate scenarios and for all four seasons. This decrease is more pronounced in the SSP-1-2.6 scenario than in the SSP-2-4.5 and SSP-5-8.5 scenarios. Under the SSP-1-2.6 scenario, only the coastal plots in the eastern region show increases in the A_{2H} variable, and these increases occur only during the JJA season. For the mid- to high-elevation areas (areas within a few kilometers of the coast or in the centre of the island), increasing trends are identified under both the SSP-2-4.5 and SSP-5-8 scenarios and over all four seasons. Under the SSP-1-2.6 scenario, only the plots located in the centre of the island (at high elevations) show systematic increases in the A_{2H} variable by the 2070–2100 period.

As with the previous results, the relative differences in mean (Fig. 7) and maximum (Fig. 8) seasonal cycle between the future and historical periods were calculated for each week of the year. The ALIZES parcels were then
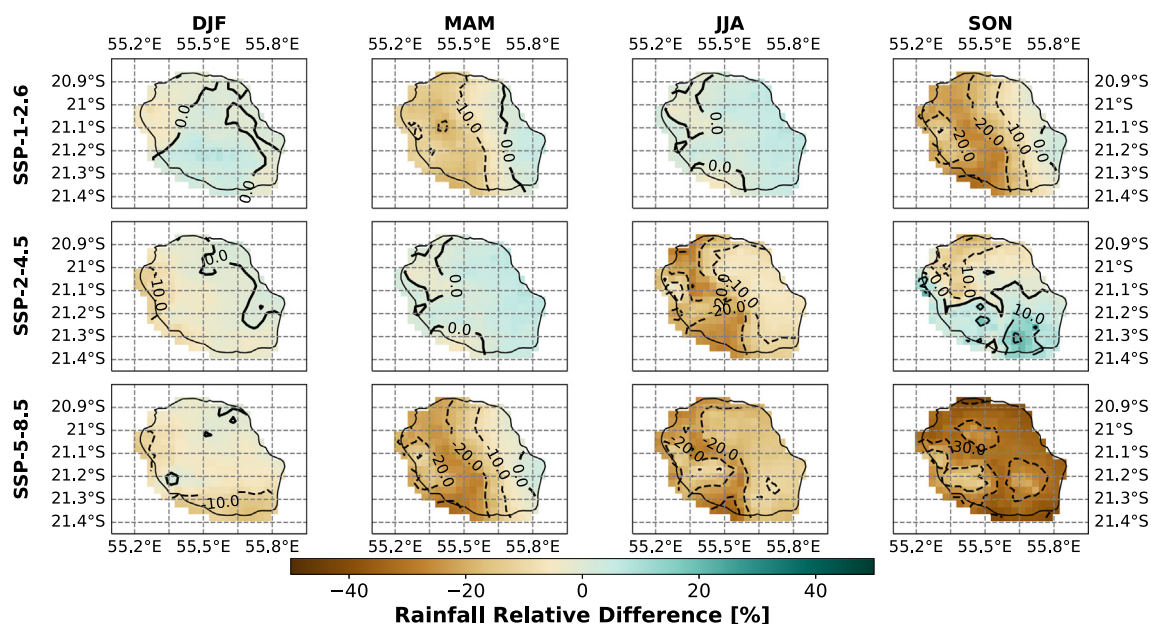

Fig. 5. Seasonal rainfall relative differences between the 2070–2100 and 1982–2012 periods. DJF: December, January and February. MAM: March, April and May. JJA: June, July and August. SON: September, October and November.
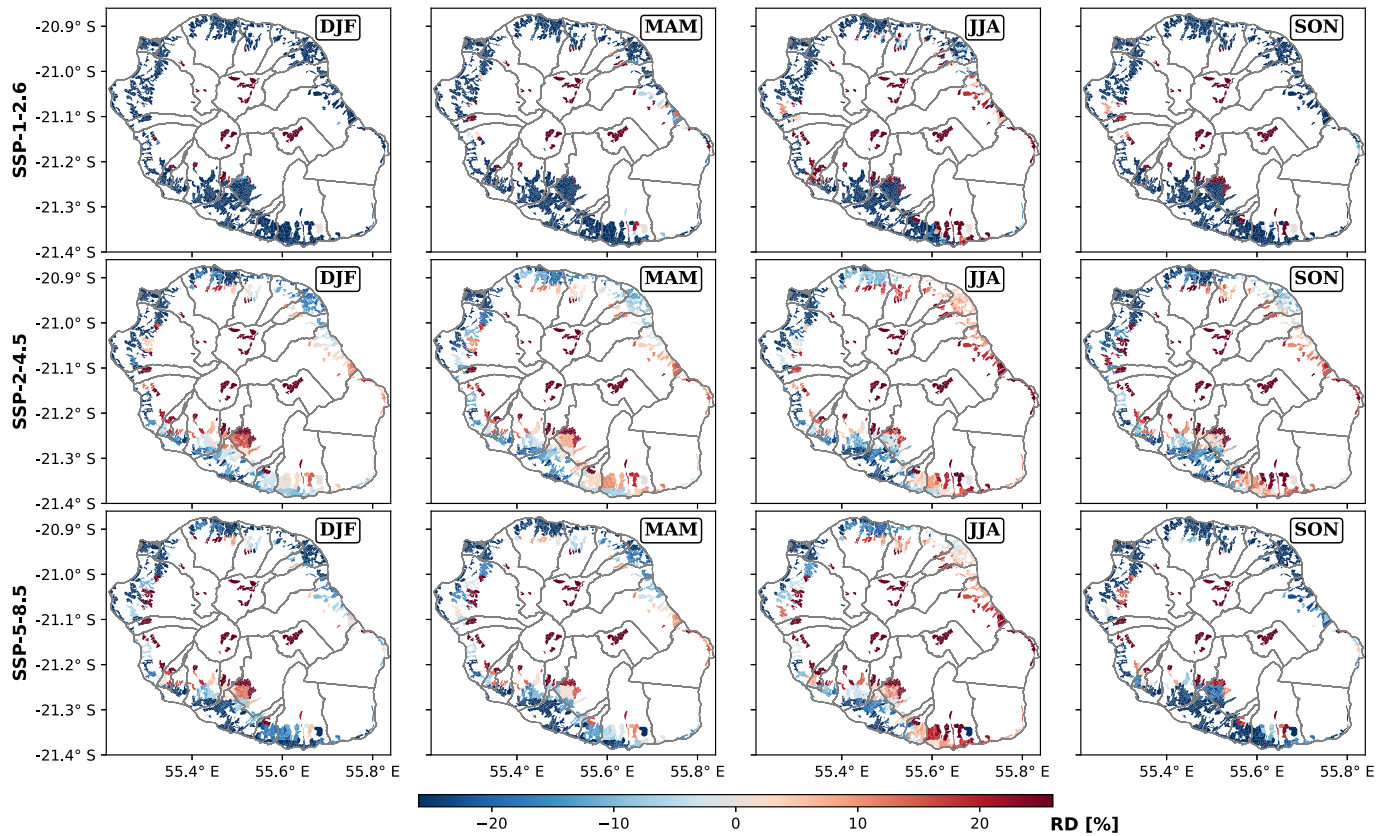
Fig. 6. Relative difference in the mean seasonal cycle of the variable A$_{2H}$ between the 2070–2100 and 1982–2012 periods.

grouped by elevation (0 to 500 m, 500 to 1000 m and over 1500 m asl) and by region of the island (north, east, west and south). These results are represented according to the three considered SSP scenarios (blue represents SSP-1-2.6, orange represents SSP-2-4.5 and red represents SSP-5-8.5).

The results confirm the previous general observations. At low elevations, decreases in the mean climatological abundance of the A$_{2H}$ variable are observed in almost all regions of the island and throughout the whole year. However, there are some positive relative difference peaks
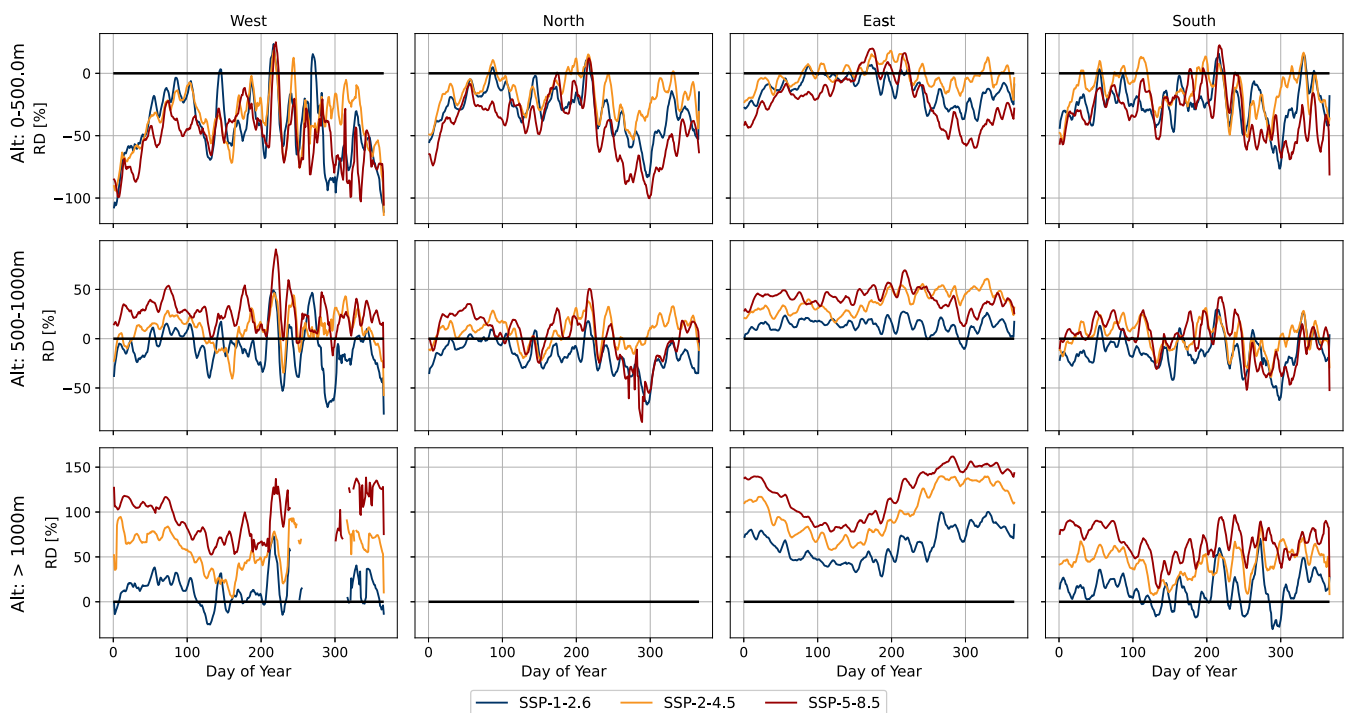

Fig. 7. Relative differences in the mean daily climatological value of the A2H variable between the 2070–2100 and 1982–2012 periods.
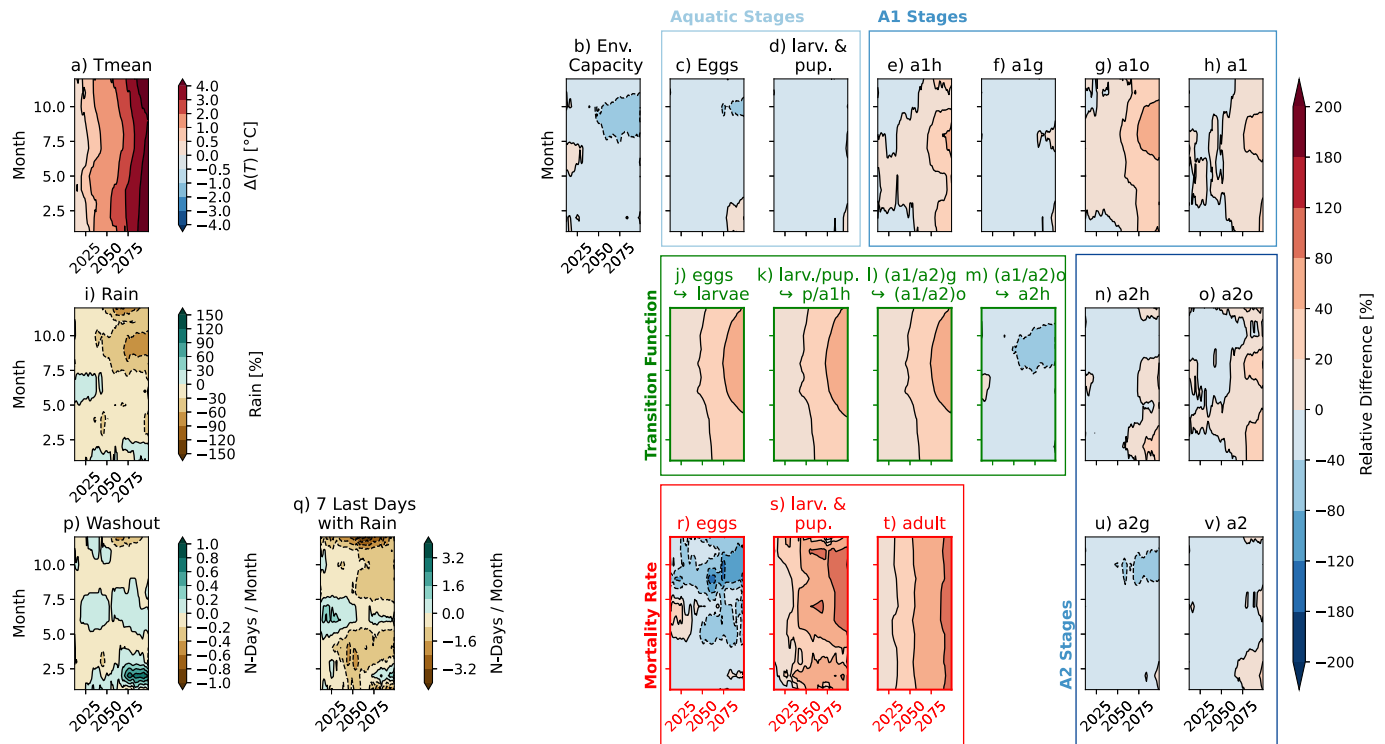
Fig. 8. Monthly percentage changes compared to the historical climatological value (1982–2012) in the mid-elevation northern region under the SSP5-8.5 scenario.

throughout the year in all four regions and under in all three low-elevation climate scenarios.

At mid-elevations, positive and negative fluctuations occur between approximately ± 50 % relative difference in the A_{2H} variable values for the western, northern and southern regions and under the three climate scenarios. In the eastern region, all three scenarios show an increase in A2H variables throughout the year. The most pessimistic scenario (SSP-5-8.5) shows the largest increase (approximately 50 % for most of the year).

At high elevations, increased values of the A_{2H} variable are observed in all regions and for most of the year. Again, the worst-case scenario shows the largest increases, with increases between approximately $+50$ and $+140$ % predicted in the western region, increases between approximately $+70$ and $+150$ % predicted in the eastern region and increases between approximately $+40$ and $+90$ % predicted in the southern region. The intermediate change scenario (SSP-2-4.5) also shows intermediate changes in the values of the A_{2H} variable. The most optimistic scenario (SSP-1-2.6) predicts the smallest changes and even some singular decreases.

Regarding the climatological maxima of the daily value (Fig. S1 in supplements) of the A_{2H} variable, similar results to the climatological averages are obtained. Nevertheless, at low elevations, the climatological maxima show larger and more frequent increases in the values of the A_{2H} variable under all climate scenarios, especially in the middle of the year for the northern and eastern regions. At mid and high elevations, the maxima increase almost year-round, under all climate scenarios and in all regions of the island. Once again, the most pessimistic scenario predicts the largest increases in the values of the A_{2H} variable.

3.2.2. Climate driver in mosquito abundance at the end of the 21st century

Fig. 8 presents a detailed analysis of the variations of entomological and meteorological variables over the seasons and the 21st century. The evolution of the difference between the monthly climatological values obtained with a 30-year moving window and those recorded in the historical period (1982–2012) for each input and output varia1ble of the ALBORUN model was calculated under the three SSP scenarios, in the three regions of the island and for the three elevations in the historical period. These results are presented in Fig. 8 for the northern mid-elevation region under the

pessimistic scenario SSP-5-8.5. The same figures for the other regions, elevations and scenarios can be found in the supplementary information. Tmean (the average daily minimal temperature and daily maximum temperature) and Rain (the daily precipitation value) are the input values obtained from ALADIN-Climate; these values determine the climatic conditions of the ALBORUN model. The entomological variables (eggs, larvae, pupa, A1x and A2x) are described in Section 2.2.1. The variables highlighted in green are the transition functions between each stage. The variables highlighted in red are the mortality rate of each stage. The transition functions from larvae to pupae and from pupae to A1H (host-seeking nulliparous females) are grouped into the same variable (Fig. 8k). The same pattern applies to larval and pupal mortality rates (Fig. 8s). The variable WASHOUT corresponds to the number of days per month that rainfall exceeded the leaching threshold of a larval site, and its relative evolution is also represented (Fig. 8p). The quantity "7 Last Days with Rain" (Fig. 8q) corresponds to the number of days per month when a minimum cumulative rainfall threshold was exceeded during the previous week.

The northern region at mid altitude for SSP-8-8.5 was chosen because it shows different periods over the century of decreasing and increasing A2H variables. Fig. 8a shows a temperature increase of approximately 4.0 °C by the end of the 21st century and throughout the year (Section 3.1.1). This increase will directly impact the transition functions of mosquitoes from the aquatic and gravid stages to the oviposition stage (Fig. 8j, k and l). The increased temperature will also increase the mortality rate of adult mosquitoes. Finally, these temperatures also play a role in the evolution of larval and pupal mortality, but the latter variable is also modulated by rainfall (Table 1) and by washouts (Fig. 8p) and by the supply of water to natural breeding sites (Fig. 8q). With respect to precipitation, we observe drying conditions corresponding to 0 and -90 % relative rainfall differences for the months of March to December and a rainfall increase between 0 and $+30$ % for the months of January and February. Rainfall has an impact on the environmental carrying capacity (Fig. 8b), which decreases throughout the year (from 0 to -40 %). Nevertheless, the direct impact of rain on the environmental carrying capacity is not systematic; in this case, the increased rainfall in January and February leads to an increase in washouts and, therefore, to a decrease in the environmental carrying capacity. Rain

also has an indirect impact on the transition function from the oviposition to host-seeking stages. When the environmental carrying capacity decreases due to drying, a decrease in the availability of egg-laying sites occurs. It then becomes difficult for female mosquitoes in the oviposition stage (A_{1O} or A_{2G}) to transition to the host-seeking stage (A_{2H}). In this case, the decrease in egg mortality (Fig. 8r) predicted for the 2070–2100 period can be attributed to the decreased cumulative rainfall at the end of the year (Fig. 8q) and the increased occurrence of washouts at the beginning of the year (Fig. 8p).

With regards to the entomological variables, the egg abundance is predicted to decrease between 0 and −80 % by the end of the century during the months from April to December and to increase between 0 and 20 % during the months from January to March. The first decrease is due to the decreased carrying capacity of the environment. The latter increase is probably due to the increased number of female mosquitoes in the oviposition stage (A_{1O} and A_{2O}) resulting from the cumulative rise in the different transition functions (Fig. 8j, k and l). Indeed, although a decrease in the abundance of aquatic stages (Fig. 8c and d) is predicted for most of the 21st century, depending on the month, a decrease or increase in the abundance of emerging and host-seeking adult females is also predicted (A_{1H}, Fig. 8e) at the beginning of the century, followed by an increase until the end of the 21st century. The A_{1H} variable increases despite the increased larva, pupa and adult mortality rates, implying that, over the long term, it is the increase in transition functions, and thus the increase in mosquito life cycle efficiency, that dominates the dynamics of A_{1H}. It can therefore be concluded that although rainfall has a dominant impact in the early 21st century, temperature will gradually become more influential on the population dynamics of *Ae. albopictus* mosquitoes.

From the gravid to the oviposition stages (A_{1G} in Fig. 8f and A2G in Fig. 8u), decreased abundances were observed. These decreases can be attributed to the increased transition function from the gravid to the oviposition stage as a consequence of the increased temperatures. The oviposition stages also increase (A_{1O} in Fig. 8g and A_{2O} in Fig. 8o), again as a consequence of the cumulative efficiency of the different transition functions.

Finally, the second stage of host-seeking adults (A_{2H} in Fig. 8n), which decreased at the beginning of the 21st century, is predicted to increase by the end of the 21st century. This trend is again an effect of the increasing efficiency of the transition between the previous life stages. In addition, the environmental carrying capacity is predicted to decrease, causing the transition function from oviposition to host-seeking to decrease. Indeed, the transition from A_{1O} to A_{2H} (or from A_{2O} to A_{2H}) is predicted to decrease throughout the 21st century. This is why the increase in A_{1H} is not of the same order as the increase in A_{2H} at the end of the 21st century.

The relative changes expected at the end of the 21st century was averaged to the annual scale and calculated for each region, elevation range and scenario. These results for rainfall, environmental carrying capacity, temperature and A_{2H} variable are presented in Table 3.

The comparison between the SSP-5-8.5 and SSP-5-8.5-Tfix simulation helps to understand the separate contribution of temperature and precipitation (Fig. 8). For a given region and elevation, several situations were obtained:

At low altitude, precipitation decreases for all regions of the island over the whole year (solid lines, Fig. 9b1/2/3/4). In the case of SSP-5-8.5, where temperatures are increasing during the 21st century (solid lines, Fig. 9c1/2/3/4), a decrease in A2H abundance is observed (solid lines, Fig. 9A1/2/3/4). However, in the case of SSP-5-8.5-Tfix (dashed lines), the abundance of A2H is almost constant throughout the 21st century. Therefore, it can be concluded that the decrease in A2H abundance is attributed to the strong increase in temperature and its impact on mortality. The negative impact of temperatures on A2H abundance at the end of the austral summer (MAM) is less significant, especially in the eastern region of the island. This period also corresponds to the epidemic peak and the end of the rainy season. The greatest impact is observed before the beginning of the austral summer (SON), at the end of the epidemic and in the dry season (Jumaux et al., 2011).

At medium and high altitudes, precipitation decreases throughout the 21st century (solid lines, Fig. 9E1/2/3/4). In the western region, A2H

increases for SSP-5-8.5 and is almost constant for SSP-5-8.5-Tfix. Therefore, increasing temperature has a positive impact on the abundance of A2H.

In the northern region, A2H decreases for SSP-5-8.5 and is almost constant for SSP-5-8.5-Tfix. Therefore, increasing temperature has a negative impact on the abundance of A2H.

In the eastern region, A2H increases for both scenarios, but the rate of change is greater and more stable for SSP-5-8.5 compared to SSP-5-8.5-Tfix. The eastern region is the rainiest and has the most rain-dependent environmental carrying capacity (Focks, 2003), so it is more susceptible to washout. It can therefore be assumed that a decrease in rainfall would reduce washout and thus decrease the mortality of aquatic stages, thus allowing for an increase in A2H. Increasing temperatures in this region also have a positive effect on A2H abundance. In the southern region, there is no significant difference between the SSP-5-8.5 and SSP-5.8.5-Tfix simulations. This conclusion is reinforced by the fact that in the dry season (SON), the decrease in precipitation does not impact the abundance of A2H by 2070–2100. Rainfall will therefore play a dominant role in this region. A summary of the meteorological variable(s) important for A2H abundance under climate change for each sub-region is proposed in the last column of Table 3.

4. Discussion

The health context of recent years has raised the importance of predicting, adapting to and mitigating health risks from infectious diseases. Furthermore, one of the major scientific challenges of this era is understanding and predicting the complex interactions between the physical and biological systems that define our environment (Kotchen and Young, 2007). Climate change and its impacts are already being felt in many biophysical systems (Kilroy, 2015; Heyder et al., 2011; Peñuelas et al., 2013). Humans generate other important impacts on their environment (Best, 2018; Foster et al., 1997; Freedman, 1995) through land use (Ostberg et al., 2015). The impacts of humans on their environment are often modulated by socioeconomic developments (Alcamo et al., 2007; Lambin and Meyfroidt, 2010), and these developments also have consequences for human health (Fuchs, 2004; Halleröd and Gustafsson, 2011). This study aimed to improve our understanding of the regional impacts of climate change on the health risk related to a major vector-borne disease, dengue, at very fine spatial (3 km) and temporal (daily) scales for a tropical island already experiencing epidemics of this disease. To this end, we focused on the impact of climate change on the population dynamics of the major dengue vector mosquito in Réunion, *Ae. albopictus*.

4.1. Main findings

Our results show both positive and negative changes in the abundance of *Ae. albopictus* on Réunion Island until the end of the 21st century. The magnitudes and signs of these changes depend on the geographical region and elevation considered and thus on the microclimate and habitat type as well as on the considered climate scenario. Decreases in the abundance of the dengue vector (from −11.5 + −6.5 % to −55 + −30 %) and thus, possibly, in the related health risk are associated with low-elevation areas where temperature increases (from approximately +1.0 °C to +3.3 °C) and precipitation decreases (from −5.3 + −2.9 % to −32.3 + −10.3 %) are expected. Increases in the abundance of the dengue vector (from 0.8 + −26.7 % to 118.9 + −33.5 %), and thus potentially in the related health risk, are associated with mid- and high-elevation regions where increased temperatures (from approximately +1.2 °C to +3.7 °C) and decreased precipitation (from −3.4 + −1.9 % to −29.2 + −10.1 %) are predicted.

Our results also highlighted the complex influence that both temperature and precipitation can have on the abundance of the *Ae. albopictus* mosquito, as these two variables can have negative as well as positive effects. Increasing temperatures can either enhance the life cycle of the mosquito and thus its abundance, or it can increase mortality rates and thus reduce its abundance. Decreases in rainfall may either promote mosquito

Table 3

Summary of the expected percent changes for the 2070–2100 period and the corresponding climatic driver by region, elevation and scenario. The blue shades correspond to a more or less pronounced decrease in A2H abundance. Red shades correspond to an increase, more or less pronounced, in temperatures or A2H abundance. Brown shades correspond to decreases in precipitation and carrying capacity.

| Region	Altitude	Scenario	Mean Monthly Percent Change in 2070-2100				Climatic Driver
			Rain [%]	$K^{l/p}$ [%]	T [°C]	A2H[%]	
West	Low	SSP-1-2.6	-21.7 ± 9.3	-24.3 ± 9.0	1.1 ± 0.1	-47.5 ± 33.7	
		SSP-2-4.5	-19.1 ± 9.5	-17.5 ± 9.3	2.0 ± 0.1	-35.2 ± 26.5	
		SSP-5-8.5	-32.3 ± 10.3	-26.5 ± 9.5	3.3 ± 0.1	-55.3 ± 30.8	Temperature
		SSP-5-8.5 (T fixed)	-32.3 ± 10.3	-26.5 ± 9.5	0.1 ± 0.1	-7.5 ± 3.3	Temperature
	Mid	SSP-1-2.6	-14.8 ± 8.0	-16.6 ± 7.6	1.1 ± 0.0	-8.7 ± 13.9	
		SSP-2-4.5	-12.4 ± 7.9	-12.4 ± 7.8	2.1 ± 0.0	11.7 ± 16.8	
		SSP-5-8.5	-22.1 ± 9.7	-18.0 ± 9.3	3.5 ± 0.1	22.1 ± 23.6	Temperature
		SSP-5-8.5 (T fixed)	-22.1 ± 9.7	-18.0 ± 9.3	0.1 ± 0.1	9.3 ± 6.3	Temperature
	High	SSP-1-2.6	-18.6 ± 7.8	-20.8 ± 7.7	1.2 ± 0.0	7.4 ± 114.5	
		SSP-2-4.5	-16.1 ± 7.9	-17.9 ± 7.2	2.1 ± 0.0	60.3 ± 131.2	
		SSP-5-8.5	-29.2 ± 10.1	-25.5 ± 9.3	3.7 ± 0.1	84.4 ± 135.2	
		SSP-5-8.5 (T fixed)	-29.2 ± 10.1	-25.5 ± 9.3	0.1 ± 0.1	-41.6 ± 10.6	
South	Low	SSP-1-2.6	-10.1 ± 6.6	-14.7 ± 7.1	1.1 ± 0.0	-23.7 ± 10.1	
		SSP-2-4.5	-11.5 ± 7.2	-11.0 ± 7.0	2.0 ± 0.1	-12.9 ± 11.0	
		SSP-5-8.5	-30.6 ± 9.1	-26.6 ± 9.7	3.4 ± 0.1	-30.6 ± 19.5	Temperature
		SSP-5-8.5 (T fixed)	-30.6 ± 9.1	-26.6 ± 9.7	0.1 ± 0.1	2.8 ± 2.4	Temperature
	Mid	SSP-1-2.6	-8.7 ± 5.5	-13.4 ± 5.8	1.2 ± 0.1	-12.9 ± 11.0	
		SSP-2-4.5	-10.8 ± 5.9	-11.2 ± 5.5	2.1 ± 0.1	5.9 ± 13.8	
		SSP-5-8.5	-29.3 ± 8.0	-25.1 ± 8.1	3.6 ± 0.1	0.8 ± 26.7	Precipitation
		SSP-5-8.5 (T fixed)	-29.3 ± 8.0	-25.1 ± 8.1	0.1 ± 0.1	13.6 ± 7.0	Precipitation
	High	SSP-1-2.6	-8.2 ± 6.3	-12.6 ± 5.8	1.2 ± 0.0	14.6 ± 9.0	
		SSP-2-4.5	-10.4 ± 7.7	-10.6 ± 5.4	2.2 ± 0.1	48.1 ± 11.7	
		SSP-5-8.5	-25.3 ± 9.1	-18.7 ± 7.4	3.7 ± 0.1	65.5 ± 15.8	Temperature and Precipitation
		SSP-5-8.5 (T fixed)	-25.3 ± 9.1	-18.7 ± 7.4	0.1 ± 0.1	35.1 ± 14.4	Temperature and Precipitation
East	Low	SSP-1-2.6	-7.2 ± 2.9	-11.1 ± 2.7	1.1 ± 0.0	-11.5 ± 6.5	
		SSP-2-4.5	-5.3 ± 2.9	-8.7 ± 2.4	1.9 ± 0.0	-18.0 ± 16.0	
		SSP-5-8.5	-20.5 ± 3.4	-21.7 ± 3.6	3.3 ± 0.1	-18.0 ± 16.0	Temperature
		SSP-5-8.5 (T fixed)	-20.5 ± 3.4	-21.7 ± 3.6	0.1 ± 0.1	3.0 ± 2.0	Temperature
	Mid	SSP-1-2.6	-5.6 ± 2.0	-7.5 ± 2.1	1.2 ± 0.0	14.7 ± 2.8	
		SSP-2-4.5	-3.4 ± 3.1	-5.1 ± 2.1	2.1 ± 0.0	36.9 ± 3.4	
		SSP-5-8.5	-18.7 ± 2.1	-15.4 ± 2.3	3.6 ± 0.0	40.1 ± 5.0	Temperature and Precipitation
		SSP-5-8.5 (T fixed)	-18.7 ± 2.1	-15.4 ± 2.3	0.1 ± 0.1	20.5 ± 9.3	Temperature and Precipitation
	High	SSP-1-2.6	-4.0 ± 3.1	-6.8 ± 2.8	1.2 ± 0.0	65.2 ± 38.5	
		SSP-2-4.5	-3.1 ± 3.1	-6.2 ± 2.4	2.1 ± 0.0	99.2 ± 64.6	
		SSP-5-8.5	-19.5 ± 3.1	-15.7 ± 3.1	3.6 ± 0.0	118.9 ± 33.5	Temperature and Precipitation
		SSP-5-8.5 (T fixed)	-19.5 ± 3.1	-15.7 ± 3.1	0.1 ± 0.1	48.5 ± 19.7	Temperature and Precipitation
North	Low	SSP-1-2.6	-14.4 ± 4.8	-18.3 ± 5.2	1.2 ± 0.0	-28.6 ± 17.1	
		SSP-2-4.5	-13.1 ± 4.5	-14.5 ± 4.8	2.1 ± 0.0	-16.4 ± 15.0	
		SSP-5-8.5	-30.1 ± 5.5	-30.11 ± 5.46	3.4 ± 0.1	-39.5 ± 22.7	Temperature
		SSP-5-8.5 (T fixed)	-30.1 ± 5.5	-30.11 ± 5.46	0.1 ± 0.1	-4.0 ± 1.5	Temperature
	Mid	SSP-1-2.6	-14.9 ± 4.4	-18.6 ± 4.7	1.2 ± 0.0	-14.7 ± 13.6	
		SSP-2-4.5	-13.2 ± 4.5	-14.41 ± 4.77	2.0 ± 0.0	9.0 ± 17.5	
		SSP-5-8.5	-28.8 ± 4.8	-28.5 ± 5.2	3.5 ± 0.1	2.9 ± 27.1	Temperature
		SSP-5-8.5 (T fixed)	-28.8 ± 4.8	-28.5 ± 5.2	0.1 ± 0.1	-3.7 ± 2.8	Temperature
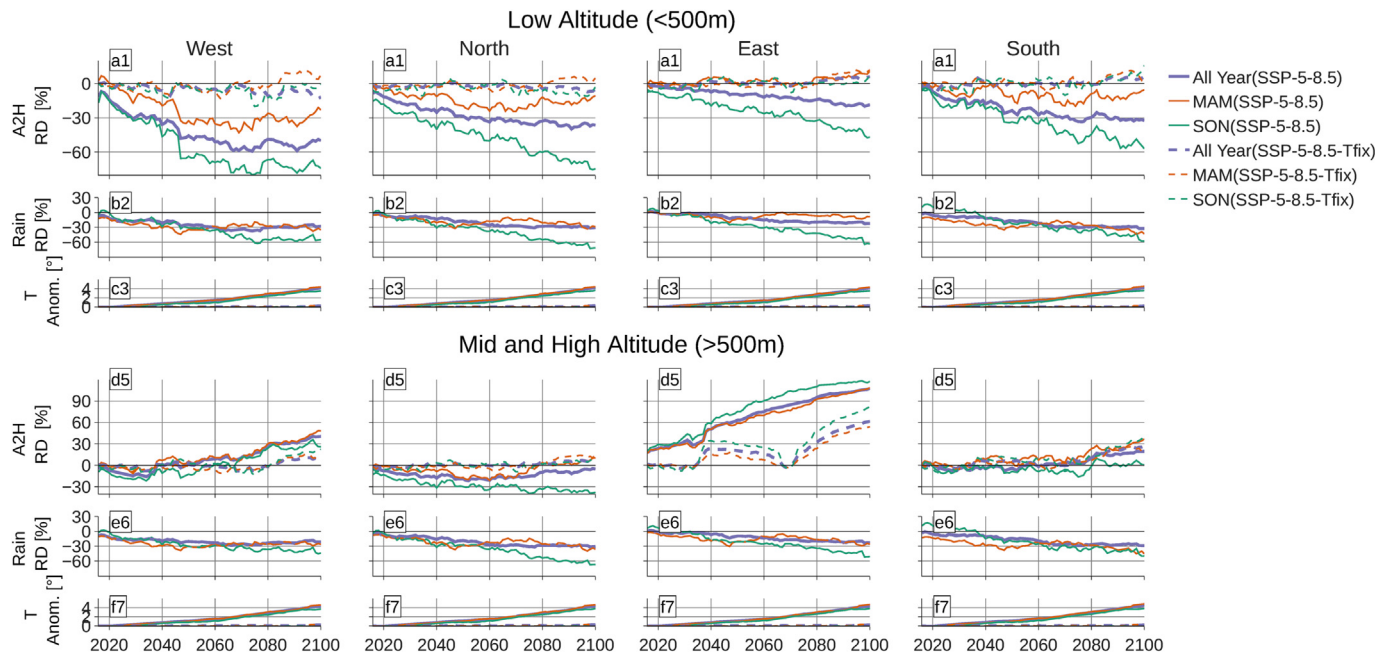
Fig. 9. Percentage changes evolution of A2H, rain, and temperature compared to the historical climatological value (1982–2012) for SSP5-8.5 and SSP5-8.5-Tfix.

abundance through reduced flushing, particularly during the rainy season and for areas with a high rainfall-dependent environmental carrying capacity, or it may have little impact on anthropogenic areas with a lower rainfall-dependent environmental carrying capacity and greater dependence on human activity. In addition, although one of these two variables may dominate the dynamics of *Ae. albopictus* during a certain climatic period, this situation may change over time.

4.2. Consistency and disparity with other studies

On the global scale, predictions of the future distributions of *Ae. albopictus* and *Ae. aegypti* by 2050 and 2080 have recently been made under different RCP climate scenarios (Kraemer et al., 2019). These researchers used habitat characteristics and climate conditions to model the future ranges of these two major vectors. To consider the expansion dynamics of each species in a given environment, the researchers also integrated human movements into their model. By 2050, both species were predicted to expand slightly beyond their current ranges. Notably, *Ae. albopictus* was predicted to expand from the eastern USA to the central USA and to the region near the border with Canada, while *Ae. aegypti* was predicted to retreat in North America. Kraemer et al. (2019) estimated that *Ae. albopictus* will have conquered its full ecological niche by 2050 and that, beyond that time, its expansion will be determined mainly by climatic and environmental variations that will make new habitats more favourable while rendering other habitats less favourable. By 2080, the researchers predicted that 197 countries will have reported the presence of the tiger mosquito compared to at least 100 countries today. Capinha et al. (2014) (Kilroy, 2015) showed that one consequences of climate change is the expansion of the spatial distribution of *Ae. aegypti* and theses macroclimatic variables will define the extent of this expansion (Capinha et al., 2014). In a study of the impact of climate change on the distribution of *Ae. albopictus* in North America, Ogden et al. (2014) also found a geographical expansion of areas suitable for the tiger mosquito and reported that the distribution of these areas depends on combined changes in temperature and precipitation (Ogden et al., 2014). The positive trends observed in our study are consistent with the work of Iwamura et al. (2020), who showed positive trends in the number of *Ae. aegypti* life cycles completed under the RCP4.5 and RCP8.5 scenarios.

In their study on *Ae. aegypti* and its presence in the mountainous regions of Mexico, Equihua et al. (2017) also showed a change in the vertical

distribution of *Ae. aegypti* (Equihua et al., 2017). The presence of this mosquito could be observed above 1200 m asl. in the warmest years. Moreover, its probability of occurrence above this elevation threshold in the distant future increased under both climate scenarios RCP 4.5 and RCP 8.5, which are approximately equivalent to the new SSP-2-4.5 and SSP-5-8.5 scenarios. Ryan et al. also predicted an increase in the number of months suitable for dengue and malaria transmission in high altitude areas (Ryan et al., 2018). The negative impact of high temperatures on mosquito abundance had also been shown in the laboratory (Teng and Apperson, 2000) and in the case of heat waves (Jia et al., 2019).

In general, our results are consistent with other work on this topic. Nevertheless, we have shown here that at the local scale, opposite changes in mosquito abundance can be observed due to negative or no impact of precipitation changes. The macro-climatic situation is therefore not sufficient to conduct successful studies on the impacts of climate change on mosquito abundance and the epidemic risk of associated vector-borne diseases.

4.3. Limitations and perspectives

4.3.1. Climate and model uncertainties

These results are subject to the uncertainties of the climate simulations and the parameterization of the ALBORUN model. Three types of uncertainties dominate the climate signals depending on the chosen climate horizon (Lehner et al., 2020):

1. 2015–2040: Uncertainties due to natural climate variabilities.
2. 2041–2070: Uncertainties related to the climate models used.
3. 2070–2100: Uncertainties related to the climate scenarios considered.

The error related to the first source of uncertainty is related to natural climate variabilities; there may be a succession of very dry or very wet seasons, or these season types may alternate. This phenomenon is linked to the chaotic nature of a dynamic system such as the atmosphere (Lorenz, 1995; Lorenz, 1963). Thus, while it is not possible to predict exactly what the weather will be like on a given day a few years or tens of years in the future, it is possible to forecast climate statistics over 30 years. This process reduces the uncertainty associated with natural climate variability and was conducted in the present study. Moreover, this uncertainty is large in the short term and decreases as the forecasted period is lengthens.

Consequently, this uncertainty dominates the climate signal in the early years of the simulation (2015–2040).

The second uncertainty, also known as the model uncertainty, arises from the response of a climate model to an external forcing. This response is not the same for all GCMs as it is a consequence of the model construction and parametrisation. To reduce this uncertainty, the results from an ensemble of climate models are generally used. In the present study, the climate simulations input to the mosquito population dynamics model were derived from a single GCM, and although this GCM has been validated (Séférian et al., 2016) and is regularly used in intercomparison exercises (Parsons et al., 2020; Fan et al., 2020), the use of an ensemble of climate projections from several GCMs would have reduced the model uncertainty (Tokarska et al., 2020; Knutti and Sedláček, 2012). Nevertheless, it was first necessary to carry out this study using a single model to simplify the problem and to analyse the interactions between the climatic and entomological variables in detail. This point of improvement will be the subject of a future study aimed at producing a set of *Ae. albopictus* population dynamics projections from a set of climate predictions derived from several GCMs.

The third uncertainty, related to the considered climate scenarios, results from the impossibility of predicting exactly the future socioeconomic and technological developments and thus the future sources of associated greenhouse gas emissions. This uncertainty can be reduced by using several possible scenarios and thus several possible emission trajectories. In this study, we used three climate scenarios considered "optimistic", "intermediate" and "pessimistic", which could be increased in the future to provide larger ensembles.

4.3.2. Ecological and environmental factors

In general, we observed that the more pessimistic the radiative scenario is, the greater the magnitudes of the expected temperatures and the greater the effect of temperature will be on *Ae. albopictus* population dynamics. It is noteworthy that the certainty of these results is qualified by the definitions of the transition functions and mortality rates (Delatte et al., 2009; Teng and Apperson, 2000; Alto and Juliano, 2001; Brady et al., 2013). These functions were obtained from experimental results carried out between 5° and 35 °C and then extrapolated to higher temperatures. However, the average temperatures expected at the end of the century in certain regions of Réunion Island, particularly at low and medium elevations, are very high and sometimes well above 35 °C or even 40 °C. There is therefore a significant source of uncertainty corresponding to the transition functions and mortality rates of *Ae. albopictus* mosquitoes at such temperatures. Moreover, some studies have shown that living organisms adapt and evolve in the context of climate change (Bradshaw and Holzapfel, 2006; Hoffmann and Daborn, 2006; Parmesan, 2006), and this finding could call into question the entomological reference parameters used herein. In general, it would therefore be important to assess the evolutionary and adaptive capacities of *Ae. albopictus*, an invasive species with significant ecological plasticity that allows it to adapt to very different environments and climates (Paupy et al., 2009), but also to assess these capacities in other mosquito species sharing the same ecological niche, such as *Ae. aegypti*, to predict the possible phenomenon of increased competition between these species (Lounibos et al., 2016) Previous work conducted on Réunion Island has highlighted that the predominance of *Ae. albopictus* on this island over *Ae. aegypti* is explained by the better demographic performance of the former species across a range of environmental conditions. Its ecological plasticity and its superior competitive ability relative to its congener may further enhance the success of its invasion on Réunion Island (Bagny Beilhe et al., 2013). In the context of the current climatic changes affecting Réunion Island, it will be interesting to follow this trend over time.

Although climate change plays an important role, other parameters also need to be taken into account when assessing the evolution of population dynamics of mosquito species such as *Ae. albopictus*. In our study, we set the rain-dependent and rain-independent environmental carrying capacities for each parcel as constant values throughout the 21st century, but

these values are likely to change with increasing population, urbanization and land use practices (water use, gardening, waste management, etc.). For example, another study showed that a large decrease in rainfall followed by a drought in Australia was linked to increased densities of the mosquito vector *Ae. aegypti* due to increased water storage (Trewin et al., 2013). In their work on *Culex quinquefasciatus*, Wang et al. (2020) showed that populations of these mosquitoes in already urbanised areas were less sensitive to increases in temperature and rainfall than those in natural areas that had become urban. For some of these urbanised areas, increased temperatures negatively affected the abundance of *Cx. quinquefasciatus*. Depending on their configuration, cities can generate significant heat island effects. Moreover, this phenomenon could be accentuated in the context of climate change (Parker, 2009). It would therefore be interesting to continue the work of the present study by varying the environmental carrying capacities according to the type of habitat, but unfortunately, no projection of future habitat type is available at the scale of Réunion Island. Furthermore, changes in human behaviour must also be considered, as these changes influence the availability and productivity of rain-independent egg-laying sites (pots, sinks, etc.) (Walker et al., 2011; Dumont and Thuilliez, 2016) and constitute a key variable affecting the prevention and control of vector-borne diseases (Roiz, 2018; Alvarado-Castro et al., 2017; Heintze et al., 2007). This variable often depends on socioeconomic and political criteria (Horstick et al., 2010; Nájera, 2001), and its influence could therefore be estimated from the different socioeconomic development scenarios associated with a single radiative forcing, for example, by comparing SSP 1-4.5, SSP 2-4.5, SSP 3-4.5, SSP 4-4.5 and SSP 4-4.5. It is important to emphasise here that factors associated with urban poverty, minimal surveillance and control capacity remain important drivers of dengue transmission in climate-sensitive regions.

The effects of the combination of urban dynamics and climate change on dengue transmission and epidemics have been extensively studied in Singapore, where the increased dengue incidence over the past 40 years, from <1000 cases in the 1980s to >14,000 cases in 2005, was estimated to be due to population growth for 86 % of the model and increased temperatures for the remaining 14% (Nabat et al., 2020). This result underlines that even without population growth, rising temperatures can lead to an increase in dengue incidence. The increase in mean temperatures may be linked to the expansion of dengue transmission to mid and higher elevations, and this threshold effect may be visible in the coming years in mountainous island regions such as Réunion Island. For example, the incidence of dengue has recently increased in mountainous countries such as Nepal (Dhimal et al., 2015). The first cases of dengue were reported in Nepal in 2006, followed by an epidemic in 2010, and the latest epidemic was reported at the end of 2017; this epidemic was still ongoing in early 2018. The main city of Kathmandu, which is over 1300 m asl, is now affected by dengue outbreaks. In another region, new evidence emerged in Puerto Rico regarding the impact of rising temperatures on the incidence of dengue. A 1 °C increase in sea surface temperatures (SSTs) was correlated with a 3.4-fold increase in dengue transmission over the 1992–2011 period (Méndez-Lázaro et al., 2014), and since warming SSTs and air surface temperatures (ASTs) are now evident, further increases in dengue incidence are expected. At the global scale, more favourable temperatures and increased rainfall by 2050 from climate change could increase the suitability of dengue in southern and western Africa, the south-eastern USA, central Mexico, northern Argentina, and inland areas of Australia. In addition, coastal cities in eastern China and Japan are projected to become more conducive to dengue vectors in 2050 (Messina et al., 2015). Interestingly, it has also been shown that more favourable climatic conditions will lead to a lengthening of the potential transmission season in many areas, particularly in the lowlands of the western Pacific and in eastern Mediterranean regions (Colón-González et al., 2021). These results must be nuanced with the fact that the population of Reunion Island is primarily concentrated on the coast. Nevertheless, the demographic and real estate pressure on the coast tends to increase the number of people settling in the highlands of the island. This increase would then reinforce the hazard associated with the epidemic risk.

5. Conclusions

In conclusion, the regional climate model, ALADIN-climate, that we used in this study showed that the temperature evolution will exhibit a linear response according to the radiative forcing conditions on Réunion Island, with an average change of approximately $+2.6°$ predicted under SSP 1-2.6, reaching $+4$ or $+5°$ under SSP 5-8.5 in 2100. The elevational temperature gradient is expected to increase in all scenarios. Regarding precipitation, the effects of climate change are not linear. It is likely that the influence of rainfall dynamics will outweigh thermodynamics. Future precipitation varies according to the scenario and season considered, but the DJF season is the only season that showed a positive trend regardless of the scenario considered. The integration of downscaled ALADIN-climate projection, from the BRIO project, with the ALBORUN model showed the combined effect of temperature and precipitation on the *Ae. albopictus* population. A shift in mosquito abundance towards higher elevations was observed under all scenarios. Coastal regions with lower elevations will experience an increase in temperatures (from approximately $+1.0$ °C to $+3.3$ °C) and a decrease in precipitation (between -5 and -32 %), leading to a decline in *Ae. albopictus* population (from -11.5 % to -55 %) and potentially reducing the risk of associated diseases. Mid- and high-elevation regions will experience an increase in temperatures ($+1.2$ °C to $+3.7$ °C) and a decrease in precipitation (-3.4 to -29.2 %), which will result in an increase in *Ae. albopictus* population of approximately 120 %.

Several sources of uncertainty exist in this study, the lack of knowledge of mosquito life cycle transition functions at high temperature or the use of fixed rather than variable environmental carrying capacities. These points can be improved in future work.

Finally, we considered only the impact of climate change on the dynamics of the different life stages of *Ae. albopictus* mosquitoes. Benkimoun et al. (2021) showed that it is possible to model the epidemiological dynamics of dengue on Réunion Island using the ALBORUN model, meteorological data and a basic reproduction model (R0) by including vector capacity, host recovery time and vector competence (Benkimoun et al., 2021). The future addition of this R0 model to climate projections will allow us to obtain better quantifications of the impacts of climate change on the risk of dengue transmission on mountainous tropical islands, such as Réunion Island.

CRediT authorship contribution statement

K. Lamy: Conceptualization, Methodology, Investigation, Writing - Original draft preparation
A. Tran: Methodology, Writing - Reviewing and Editing
T. Portafaix: Writing - Reviewing and Editing
M.D. Leroux: Methodology, Writing - Reviewing and Editing
T. Baldet: Writing - Reviewing and Editing

Data availability

Data will be made available on request.

Declaration of competing interest

Appendix A. Supplementary data

Supplementary data to this article can be found online at https://doi.org/10.1016/j.scitotenv.2023.162484.

References

Alcamo, J., Flörke, M., Märker, M., 2007. Future long-term changes in global water resources driven by socio-economic and climatic changes. Hydrol. Sci. J. 52.

Alto, B.W., Juliano, S.A., 2001. Precipitation and temperature effects on populations of Aedes albopictus (Diptera: Culicidae): implications for range expansion. J. Med. Entomol. 38.

Alvarado-Castro, V., et al., 2017. Assessing the effects of interventions for Aedes aegypti control: systematic review and meta-analysis of cluster randomised controlled trials. BMC Public Health 17.

Bagny Beilhe, L., Delatte, H., Juliano, S.A., Fontenille, D., Quilici, S., 2013. Ecological interactions in aedes species on Reunion Island. Med. Vet. Entomol. 27.

Benkimoun, S., et al., 2021. Dynamic mapping of dengue basic reproduction number. Results Phys. 29, 104687.

Best, J., 2018. Anthropogenic stresses on the world's big rivers. Nat. Geosci. 12, 7–21.

Bhatt, S., et al., 2013. The global distribution and burden of dengue. Nature 496.

Bindoff, N.L., 2013. In: Climate Change, I. P (Ed.), Detection and Attribution of Climate Change: from Global to Regional. in Climate Change 2013 - The Physical Science Basis. Cambridge University Press, pp. 867–952 https://doi.org/10.1017/cbo9781107415324.022.

Bonfils, C.J.W., et al., 2020. Human influence on joint changes in temperature, rainfall and continental aridity. Nat. Clim. Chang. 10, 726–731.

Bonnin, L., Tran, A., Herbreteau, V., Marcombe, S., Boyer, S., Mangeas, M., Menkes, C., 2022. Predicting the effects of climate change on dengue vector densities in Southeast Asia through process-based modeling. Environ Health Perspect 130, 127002. https://doi.org/10.1289/EHP11068.

Bradshaw, W.E., Holzapfel, C.M., 2006. Evolutionary response to rapid climate change. Science 1979 (312), 1477–1478.

Brady, O.J., et al., 2013. Modelling adult Aedes aegypti and Aedes albopictus survival at different temperatures in laboratory and field settings. Parasit. Vectors 6.

Brown, H.E., Barrera, R., Comrie, A.C., Lega, J., 2017. Effect of temperature thresholds on modeled Aedes aegypti (Diptera: Culicidae) population dynamics. J. Med. Entomol. 54.

Cailly, P., et al., 2012. A climate-driven abundance model to assess mosquito control strategies. Ecol. Model. 227, 7–17.

Capinha, C., Rocha, J., Sousa, C.A., 2014. Macroclimate determines the global range limit of Aedes aegypti. EcoHealth 11, 420–428.

Chadwick, R., Good, P., Willett, K., 2016. A simple moisture advection model of specific humidity change over land in response to SST warming. J. Clim. 29, 7613–7632.

Chan, M., Johansson, M.A., 2012. The incubation periods of dengue viruses. PLoS One 7.

Colón-González, F.J., et al., 2021. Projecting the risk of mosquito-borne diseases in a warmer and more populated world: a multi-model, multi-scenario intercomparison modelling study. Lancet Planet Health 5.

Coulanges, P., Clercy, Y., Jousset, F.X., Rodhain, F., Hannoun, C., 1979. Dengue at Reunion: isolation of a strain at the pasteur Institute of Madagascar. Bull. Soc. Pathol. Exot. Filiales 72.

Daniel, M., et al., 2018. Benefits of explicit urban parameterization in regional climate modeling to study climate and city interactions. Clim. Dyn. 52, 2745–2764.

Delatte, H., Gimonneau, G., Triboire, A., Fontenille, D., 2009. Influence of temperature on immature development, survival, longevity, fecundity, and gonotrophic cycles of Aedes albopictus, vector of chikungunya and dengue in the Indian Ocean. J. Med. Entomol. 46, 33–41.

Dhimal, M., Ahrens, B., Kuch, U., 2015. Climate change and spatiotemporal distributions of vector-borne diseases in Nepal - a systematic synthesis of literature. PLoS ONE 10. https://doi.org/10.1371/journal.pone.0129869 Preprint at.

Dieng, H., et al., 2012. The effects of simulated rainfall on immature population dynamics of Aedes albopictus and female oviposition. Int. J. Biometeorol. 56.

Dumont, Y., Thuilliez, J., 2016. Human behaviors: a threat to mosquito control? Math. Biosci. 281, 9–23.

Equihua, M., et al., 2017. Establishment of Aedes aegypti (L.) in mountainous regions in Mexico: increasing number of population at risk of mosquito-borne disease and future climate conditions. Acta Trop. 166, 316–327.

Eritja, R., Palmer, J.R.B., Roiz, D., Sanpera-Calbet, I., Bartumeus, F., 2017. Direct evidence of adult Aedes albopictus dispersal by car. Sci. Rep. 7.

Fan, X., Miao, C., Duan, Q., Shen, C., Wu, Y., 2020. The performance of CMIP6 versus CMIP5 in simulating temperature extremes over the global land surface. J. Geophys. Res. Atmos. 125.

Faridah, L., et al., 2022. Temporal correlation between urban microclimate, vector mosquito abundance, and dengue cases. J. Med. Entomol. 59.

Focks, D., 2003. A Review of Entomological Sampling Methods and Indicators for dengue Vectors. Special Program for Research and Training in Tropical Diseases (TDR). UNICEF, UNDP, World Bank, WHO Special Programme for Research and Training in Tropical Diseases. 28.

Foster, D.R., Aber, J.D., Melillo, J.M., Bowden, R.D., Bazzaz, F.A., 1997. Forest response to disturbance and anthropogenic stress. Bioscience 47, 437–445.

Freedman, B., 1995. Environmental Ecology: The Ecological Effects of Pollution, Disturbance, and Other Stresses. Elsevier.

Fuchs, V.R., 2004. Reflections on the socio-economic correlates of health. J. Health Econ. 23, 653–661.

Gloria-Soria, A., Brown, J.E., Kramer, V., Hardstone Yoshimizu, M., Powell, J.R., 2014. Origin of the dengue fever mosquito, Aedes aegypti, in California. PLoS Negl. Trop. Dis. 8.

Hafsia, S., Haramboure, M., Wilkinson, D.A., Baldet, T., Yemadje-Menudier, L., Vincent, M., Tran, A., Atyame, C., Mavingui, P., 2022. Overview of dengue outbreaks in the south western indian and analysis of factors involved in the shift towards endemicity in Reunion Island: a systematic review. PLoS Negl. Trop. 16, 1–16.

Halleröd, B., Gustafsson, J.-E., 2011. A longitudinal analysis of the relationship between changes in socio-economic status and changes in health. Soc Sci Med 72, 116–123.

Heintze, C., Garrido, M.V., Kroeger, A., 2007. What do community-based dengue control programmes achieve? A systematic review of published evaluations. Trans. R. Soc. Trop. Med. Hyg. 101, 317–325.

Heyder, U., Schaphoff, S., Gerten, D., Lucht, W., 2011. Risk of severe climate change impact on the terrestrial biosphere. Environ. Res. Lett. 6, 34036.

Hoffmann, A.A., Daborn, P.J., 2006. Towards genetic markers in animal populations as biomonitors for human-induced environmental change. Ecol. Lett. 10, 63–76.

Horstick, O., Runge-Ranzinger, S., Nathan, M.B., Kroeger, A., 2010. Dengue vector-control services: how do they work? A systematic literature review and country case studies. Trans. R. Soc. Trop. Med. Hyg. 104, 379–386.

Insee, 2022. Estimations de population par sexe et âge au 1er janvier 2022.

IPCC, 2013. Intergovernmental Panel on Climate Change Working Group I. Climate Change 2013: The Physical Science Basis. Long-term Climate Change: Projections, Commitments and Irreversibility. Cambridge University Press, New York.

IPCC, 2021. Climate Change 2021: The Physical Science Basis. The Physical Science Basis. Contribution of Working Group I to the Sixth Assessment Report of the Intergovernmental Panel on Climate Change. Cambridge University Press.

Iwamura, T., Guzman-Holst, A., Murray, K.A., 2020. Accelerating invasion potential of disease vector Aedes aegypti under climate change. Nat. Commun. 11.

Jia, P., Liang, L., Tan, X., Chen, J., Chen, X., 2019. Potential effects of heat waves on the population dynamics of the dengue mosquito Aedes albopictus. PLoS Negl. Trop. Dis. 13.

Juliano, S.A., 2007. Population dynamics. J. Am. Mosq. Control Assoc. 23, 265–275.

Jumaux, G., Quetelard, H., Roy, D., 2011. Atlas climatique de la Réunion. Direction interrégionale de la Réunion, Météo-France.

Kamal, M., Kenawy, M.A., Rady, M.H., Khaled, A.S., Samy, A.M., 2018. Mapping the global potential distributions of two arboviral vectors Aedes aegypti and Ae. Albopictus under changing climate. PLoS One 13.

Kilpatrick, A.M., Randolph, S.E., 2012. Drivers, dynamics, and control of emerging vector-borne zoonotic diseases. Lancet 380, 1946–1955.

Kilroy, G., 2015. A review of the biophysical impacts of climate change in three hotspot regions in Africa and Asia. Reg. Environ. Chang. 15, 771–782.

Kles, V., Michault, A., Rodhain, F., Mevel, F., Chastel, C., 1994. A serological survey regarding flaviviridae infections on the island of Réunion (1971–1989). Bull. Soc. Pathol. Exot. 87.

Knutson, T.R., Zeng, F., 2018. Model assessment of observed precipitation trends over land regions: detectable human influences and possible low bias in model trends. J. Clim. 31, 4617–4637.

Knutti, R., Sedláček, J., 2012. Robustness and uncertainties in the new {CMIP}5 climate model projections. Nat. Clim. Chang. 3, 369–373.

Kotchen, M.J., Young, O.R., 2007. Meeting the challenges of the anthropocene: towards a science of coupled human–biophysical systems. Glob. Environ. Chang. Hum. Policy Dimens. 17, 149–151.

Kovats, R.S., Campbell-Lendrum, D.H., McMichael, A.J., Woodward, A., Cox, J.S.H., 2001. Early effects of climate change: do they include changes in vector-borne disease? Philos. Trans. R. Soc., B 356.

Kraemer, M.U.G., et al., 2015. The global distribution of the arbovirus vectors Aedes aegypti and ae. Albopictus. elife 4.

Kraemer, M.U.G., et al., 2019. Past and future spread of the arbovirus vectors Aedes aegypti and Aedes albopictus. Nat. Microbiol. 4.

Kröckel, U., Rose, A., Eiras, Á.E., Geier, M., 2006. New tools for surveillance of adult yellow fever mosquitoes: comparison of trap catches with human landing rates in an urban environment. J. Am. Mosq. Control Assoc. 22.

Kumar, R., Pande, V., Pasi, S., Ojha, V.P., Dhiman, R.C., 2018. Air versus water temperature of aquatic habitats in Delhi: implications for transmission dynamics of Aedes aegypti. Geospat. Health 13.

Lacroix, R., Delatte, H., Hue, T., Reiter, P., 2009. Dispersal and survival of male and female aedes albopictus (Diptera: Culicidae) on réunion island. J. Med. Entomol. 46.

Lambin, E.F., Meyfroidt, P., 2010. Land use transitions: socio-ecological feedback versus socio-economic change. Land Use Policy 27, 108–118.

Larsen, L., 2015. Urban climate and adaptation strategies. Front. Ecol. Environ. 13. https://doi.org/1890/150103.

Lehner, F., et al., 2020. Partitioning climate projection uncertainty with multiple large ensembles and CMIP5/6. Earth Syst. Dyn. 11, 491–508.

Leroux, M.D., 2021. Regional Climate Projections and Associated Climate Services in the Southwest Indian Ocean Basin. https://doi.org/10.5194/egusphere-egu21-7029.

Li, Y., et al., 2014. Urbanization increases Aedes albopictus larval habitats and accelerates mosquito development and survivorship. PLoS Negl. Trop. Dis. 8.

Li, X., et al., 2015. Trend and seasonality of land precipitation in observations and CMIP5 model simulations. Int. J. Climatol. 36, 3781–3793.

Liu, C., Allan, R.P., 2013. Observed and simulated precipitation responses in wet and dry regions 1850–2100. Environ. Res. Lett. 8, 34002.

Liu-Helmersson, J., et al., 2016. Climate change and aedes vectors: 21st century projections for dengue transmission in Europe. EBioMedicine 7, 267–277.

Lorenz, E.N., 1963. Deterministic nonperiodic flow. J. Atmos. Sci. 20, 130–141.

Lorenz, E.N., 1995. Predictability: a problem partly solved. Seminar on Predictability, 4-8 September 1995. vol. 1. ECMWF, pp. 1–18 Preprint at.

Lounibos, L.P., Bargielowski, I., Carrasquilla, M.C., Nishimura, N., 2016. Coexistence of Aedes aegypti and Aedes albopictus (Diptera: Culicidae) in peninsular Florida two decades after competitive displacements. J. Med. Entomol. 53.

Lowe, R., et al., 2020. Emerging arboviruses in the urbanized Amazon rainforest. BMJ 371.

Lowe, R., et al., 2021. Combined effects of hydrometeorological hazards and urbanisation on dengue risk in Brazil: a spatiotemporal modelling study. Lancet Planet Health 5.

Lucas, B., et al., 2022. Predicting the effects of climate change on dengue vector densities in Southeast Asia through process-based modeling. Environ. Health Perspect. 130, 127002.

Lwande, O.W., 2020. Globe-trotting Aedes aegypti and Aedes albopictus: risk factors for arbovirus pandemics. Vector Borne Zoonotic Dis. 20. https://doi.org/10.1089/vbz.2019.2486 Preprint at.

Méndez-Lázaro, P., Muller-Karger, F.E., Otis, D., McCarthy, M.J., Peña-Orellana, M., 2014. Assessing climate variability effects on dengue incidence in San Juan, Puerto Rico. Int. J. Environ. Res. Public Health 11.

Messina, J.P., et al., 2015. The many projected futures of dengue. Nat. Rev. Microbiol. 13, 230–239.

Michelangeli, P.A., Vrac, M., Loukos, H., 2009. Probabilistic downscaling approaches: application to wind cumulative distribution functions. Geophys. Res. Lett. 36.

Murdock, C.C., Evans, M.V., McClanahan, T.D., Miazgowicz, K.L., Tesla, B., 2017. Fine-scale variation in microclimate across an urban landscape shapes variation in mosquito population dynamics and the potential of Aedes albopictus to transmit arboviral disease. PLoS Negl. Trop. Dis. 11.

Murray, N.E.A., Quam, M.B., Wilder-Smith, A., 2013. Epidemiology of dengue: past, present and future prospects. Clin. Epidemiol. 5. https://doi.org/10.2147/CLEP.S34440 Preprint at.

Nabat, P., et al., 2020. Modulation of radiative aerosols effects by atmospheric circulation over the Euro-Mediterranean region. Atmos. Chem. Phys. 20, 8315–8349.

Nájera, J.A., 2001. Malaria control: achievements, problems and strategies. Parassitologia 43, 1–89.

O'Neill, B.C., et al., 2016. The scenario model intercomparison project (ScenarioMIP) for CMIP6. Geosci. Model Dev. 9, 3461–3482.

Ogden, N.H., Milka, R., Caminade, C., Gachon, P., 2014. Recent and projected future climatic suitability of North America for the asian tiger mosquito Aedes albopictus. Parasit. Vectors 7.

Oliver, M.A., Webster, R., 1990. Kriging: a method of interpolation for geographical information systems. Int. J. Geogr. Inf. Syst. 4.

Ostberg, S., Schaphoff, S., Lucht, W., Gerten, D., 2015. Three centuries of dual pressure from land use and climate change on the biosphere. Environ. Res. Lett. 10, 44011.

Pachka, H., 2016. Rift Valley fever vector diversity and impact of meteorological and environmental factors on Culex pipiens dynamics in the Okavango Delta, Botswana. Parasit. Vectors 9.

Paixão, E.S., Teixeira, M.G., Rodrigues, L.C., 2018. Zika, chikungunya and dengue: the causes and threats of new and reemerging arboviral diseases. BMJ Glob. Health 3.

Parker, D.E., 2009. Urban heat island effects on estimates of observed climate change. WIREs Clim. Change 1, 123–133.

Parmesan, C., 2006. Ecological and evolutionary responses to recent climate change. Annu. Rev. Ecol. Evol. Syst. 37, 637–669.

Parsons, L.A., Brennan, M.K., Wills, R.C.J., Proistosescu, C., 2020. Magnitudes and spatial patterns of interdecadal temperature variability in CMIP6. Geophys. Res. Lett. 47.

Patz, J.A., Martens, W.J.M., Focks, D.A., Jetten, T.H., 1998. Dengue fever epidemic potential as projected by general circulation models of global climate change. Environ. Health Perspect. 106.

Paupy, C., Delatte, H., Bagny, L., Corbel, V., Fontenille, D., 2009. Aedes albopictus, an arbovirus vector: from the darkness to the light. Microbes Infect. 11.

Peñuelas, J., et al., 2013. Evidence of current impact of climate change on life: a walk from genes to the biosphere. Glob. Chang. Biol. 19, 2303–2338.

Roiz, D., 2018. Integrated Aedes management for the control of Aedes-borne diseases. PLoS Negl. Trop. Dis. 12. https://doi.org/10.1371/journal.pntd.0006845 Preprint at.

Ryan, S.J., Carlson, C.J., Mordecai, E.A., Johnson, L.R., 2018. Global expansion and redistribution of aedes-borne virus transmission risk with climate change. PLoS Negl. Trop. Dis. 13.

Santé Publique France, 2021. DENGUE. Point épidémiologique hebdomadaire du 7 décembre 2021. Santé publique France-Réunion.

Santé Publique France, 2022. Surveillance de la dengue à La Réunion. Point au 15 juin 2022.

Sauer, F.G., Grave, J., Lühken, R., Kiel, E., 2021. Habitat and microclimate affect the resting site selection of mosquitoes. Med. Vet. Entomol. 35.

Schuffenecker, I., et al., 2006. Genome microevolution of chikungunya viruses causing the Indian Ocean outbreak. PLoS Med. 3.

Schurer, A.P., Ballinger, A.P., Friedman, A.R., Hegerl, G.C., 2020. Human influence strengthens the contrast between tropical wet and dry regions. Environ. Res. Lett. 15.

Séférian, R., et al., 2016. Development and evaluation of CNRM earth system model-CNRM-ESM1. Geosci. Model Dev. 9.

Séférian, R., et al., 2019. Evaluation of CNRM earth system model, CNRM-ESM2-1: role of earth system processes in present-day and future climate. J. Adv. Model. Earth Syst. 11.

Semenza, J.C., et al., 2014. International dispersal of dengue through air travel: importation risk for Europe. PLoS Negl. Trop. Dis. 8.

Solman, S.A., Orlanski, I., 2016. Climate change over the extratropical southern hemisphere: the tale from an ensemble of reanalysis datasets. J. Clim. 29.

Strasberg, D., et al., 2005. An assessment of habitat diversity and transformation on La Réunion Island (Mascarene Islands, Indian Ocean) as a basis for identifying broad-scale conservation priorities. Biodivers. Conserv. 14.

Struchiner, C.J., Rocklöv, J., Wilder-Smith, A., Massad, E., 2015. Increasing dengue incidence in Singapore over the past 40 years: population growth, climate and mobility. PLoS One 10.

Tatem, A.J., Hay, S.I., Rogers, D.J., 2006. Global traffic and disease vector dispersal. Proc. Natl. Acad. Sci. U. S. A. 103.

Teng, H.J., Apperson, C.S., 2000. Development and survival of immature Aedes albopictus and Aedes triseriatus (Diptera: Culicidae) in the laboratory: effects of density, food, and competition on response to temperature. J. Med. Entomol. 37.

Tian, B., Dong, X., 2020. The double-ITCZ bias in CMIP3, CMIP5, and CMIP6 models based on annual mean precipitation. Geophys. Res. Lett. 47.

Tokarska, K.B., et al., 2020. Past warming trend constrains future warming in CMIP6 models. Sci. Adv. 6.

Tran, A., et al., 2013. A rainfall- and temperature-driven abundance model for Aedes albopictus populations. Int. J. Environ. Res. Public Health 10, 1698–1719.

Tran, A., et al., 2020. Complementarity of empirical and processbased approaches to modelling mosquito population dynamics with Aedes albopictus as an example-application to the development of an operational mapping tool of vector populations. PLoS One 15, 1–21.

Trewin, B.J., Kay, B.H., Darbro, J.M., Hurst, T.P., 2013. Increased container-breeding mosquito risk owing to drought-induced changes in water harvesting and storage in Brisbane, Australia. Int. Health 5.

Vavassori, L., Saddler, A., Müller, P., 2019. Active dispersal of Aedes albopictus: a mark-release-recapture study using self-marking units. Parasit. Vectors 12.

Vincent, M., et al., 2019. From the threat to the large outbreak: dengue on Reunion Island, 2015 to 2018. Eurosurveillance 24.

Vrac, M., et al., 2012. Dynamical and statistical downscaling of the French Mediterranean climate: uncertainty assessment. Nat. Hazards Earth Syst. Sci. 12.

Walker, K.R., Joy, T.K., Ellers-Kirk, C., Ramberg, F.B., 2011. Human and environmental factors affecting Aedes aegypti distribution in an arid urban environment. J. Am. Mosq. Control Assoc. 27, 135–141.

Wan, H., Zhang, X., Zwiers, F., Min, S.-K., 2014. Attributing northern high-latitude precipitation change over the period 1966–2005 to human influence. Clim. Dyn. 45, 1713–1726.

Wang, Y., Yim, S.H.L., Yang, Y., Morin, C.W., 2020. The effect of urbanization and climate change on the mosquito population in the Pearl River Delta region of China. Int. J. Biometeorol. 64.

World Health Organization, 2014. WHO Factsheet Vector-borne Diseases. Factsheet Number 387.

Xu, L., et al., 2017. Climate variation drives dengue dynamics. Proc. Natl. Acad. Sci. U. S. A. 114.